DOI:10.1158/1078-0432.CCR-08-1305

Obstructing Shedding of the Immunostimulatory MHC Class I Chain–Related Gene B Prevents Tumor Formation

Jennifer D. Wu,[1] Catherine L. Atteridge,[1] Xuanjun Wang,[1] Tsukasa Seya,[3] and Stephen R. Plymate[1,2]

Abstract

Purpose: Clinical observations have suggested that shedding of the MHC class I chain–related molecule (MIC) may be one of the mechanisms by which tumors evade host immunosurveillance and progress. However, this hypothesis has never been proven. In this study, we tested this hypothesis using a prostate tumor model and investigated the effect of shedding of MIC on tumor development.

Experimental Design: We generated a shedding-resistant noncleavable form of MICB (MICB.A2). We overexpressed MICB.A2, the wild-type MICB, and the recombinant soluble MICB (rsMICB) in mouse prostate tumor TRAMP-C2 (TC2) cells and implanted these cells into severe combined immunodeficient mice.

Results: No tumors were developed in animals that were implanted with TC2-MICB.A2 cells, whereas all the animals that were implanted with TC2, TC2-MICB, or TC2-rsMICB cells developed tumors. When a NKG2D-specific antibody CX5 or purified rsMICB was administered to animals before tumor implantation, all animals that were implanted with TC2-MICB.A2 cells developed tumors. *In vitro* cytotoxicity assay revealed the loss of NKG2D-mediated natural killer cell function in these prechallenged animals, suggesting that persistent levels of soluble MICB in the serum can impair natural killer cell function and thus allow tumor growth.

Conclusions: These data suggest that MIC shedding may contribute significantly to tumor formation by transformed cells and that inhibition of MIC shedding to sustain the NKG2D receptor-MIC ligand recognition may have potential clinical implication in targeted cancer treatment.

Expression of murine NKG2D ligands on tumor cells has been shown to be effective in activating natural killer (NK)-mediated tumor elimination experimentally (1–4). In murine systems, identified NKG2D ligands include the retinoic acid early inducible family of proteins RAE-1 (1, 2), the minor histocompatibility antigen H60 (1, 2), and the murine ULBP-like transcript 1 (4, 5). Cells expressing these molecules are sensitive to the cytotoxicity of mouse NK cells. Ectopic expression of RAE-1 and H60 results in rejection of tumor cell lines expressing normal levels of MHC I molecule (2–4). Immunodepletion and other experiments showed that the tumor rejection is due to NK and CD8 T cells (2, 3). NKG2D neutralization *in vivo* enhances host sensitivity to carcinogen-induced spontaneous tumor initiation (6). These studies have proven the principle function of the NKG2D ligand receptor-mediated NK cell immunity in tumor rejection.

In humans, the MHC class I chain–related molecule MICA and MICB (generally termed as MIC) are the most investigated NKG2D ligands, which were proposed to play roles in tumor rejection (7–9). MIC is rarely expressed by normal human tissues but induced in most human epithelial tumors (10–13). Expression of MIC on the tumor cell surface can markedly enhance the sensitivity of tumor cells to NK cells *in vitro* and has been shown to inhibit the growth of human gliomas or small lung carcinomas in experimental models (14, 15). These studies suggested that NK cells can potentially eliminate MIC-positive tumor cells in cancer patients. However, as clinically observed, most of the human epithelial tumors are found to be MIC-positive rather than MIC-negative (10–13), which suggests the functional compromise of the MIC ligand-NKG2D receptor system in cancer patients to permit the growth of MIC-positive tumor cells. We and others have shown that tumor-derived soluble MIC as a result of tumor shedding is one of the factors causing the ineffectiveness of NKG2D-mediated immunity in cancer patients (13, 16–21). *In vitro* studies have shown that engagement of soluble MICA to NKG2D results in marked reduction in surface NKG2D expression on NK and T cells (13, 16, 21). Thus, soluble MIC is believed to induce down-modulation of NKG2D expression on systemic and tumor-infiltrated NK and T cells and thus result in functional impairment of NK and T cells in MIC-positive cancer patients (13, 16, 17). Reduction in the density of MIC expressed on the tumor cell surface due to MIC shedding from tumors is also proposed to be one of the mechanisms for tumor evasion (21).

Authors' Affiliations: [1]Department of Medicine, University of Washington; [2]Geriatric Research, Education and Clinical Center, Veterans Affairs Puget Sound Health Care System, Seattle, Washington and [3]Department of Microbiology and Immunology, Hokkaido University Graduate School of Medicine, Sapporo, Japan

Received 5/19/08; revised 8/12/08; accepted 8/20/08.

Grant support: DOD-USMRC New Investigators Grant W81XWH-04-1-0577 and IDEA Development Award W81XWH-06-1-0014, NW Prostate SPORE Program, and NIH Temin Award 1K01CA116002 (J.D.Wu).

The costs of publication of this article were defrayed in part by the payment of page charges. This article must therefore be hereby marked *advertisement* in accordance with 18 U.S.C. Section 1734 solely to indicate this fact.

Requests for reprints: Jennifer D. Wu, Department of Medicine, University of Washington, 325 9th Avenue, Box 359625, Seattle, WA 98104. Phone: 206-341-5349; Fax: 206-341-5302; E-mail: wuj@u.washington.edu.

doi:10.1158/1078-0432.CCR-08-1305

DOI:10.1158/1078-0432.CCR-08-1305

Translational Relevance

In humans, the MHC class I chain-related molecules MICA and MICB (generally termed MIC) are frequently found expressed on epithelial-originated tumor cells. MIC is a ligand for the activating NK cell receptor NKG2D. Engagement of tumor-expressed MIC to NKG2D can activate NK cell tumor-lytic activity *in vitro*. Thus, expression of MIC on tumor cells is proposed to play a significant role in tumor immunosurveillance. However, as observed in many cancer patients, majority of the tumors remain MIC positive, suggesting the ineptness of the NKG2D-mediated NK cell function. We and others have shown that shedding of MIC by tumor cells can impair NK cell function in cancer patients. These clinical studies prompted the hypothesis that tumor shedding of MIC may be one of the mechanisms by which MIC-positive tumors evade NK cell immunosurveillance and progress. This study tested this hypothesis *in vivo* using a prostate tumor model and for the first time showed that interfering with shedding of MIC could prevent tumor formation. Our study suggests that shedding of MIC may contribute significantly to tumor formation by transformed cells and thus inhibiting tumor shedding of MIC may have potential therapeutic implication in targeted cancer therapy.

These compelling clinical data suggest that MIC shedding from tumor cells is likely associated with tumor progression, which has prompted the hypothesis that tumor shedding of MIC is the mechanism by which MIC-positive tumors evade NK cell immunosurveillance and progress in cancer patients. However, it is impossible to test this hypothesis clinically. Taking the advantage that human MICB can be recognized by mouse NKG2D (22, 23) and that only the extracellular $\alpha1\alpha2$ domain of MIC interacts with NKG2D (24–26), here we test the hypothesis experimentally that shedding of MIC permits tumor growth and that sustained interaction between NKG2D and membrane-integrated form of MIC can cause tumor rejection. Using a well-characterized prostate tumor model TRAMP-C2 (TC2; ref. 27), we show for the first time that expression of the shedding-resistant but not the natural form of MICB prevents tumor formation by transformed cells.

Materials and Methods

Cells. TC2 cell line (gift of Dr. N.M. Greenberg, Fred Hutchinson Cancer Research Center) was maintained in DMEM as described (27). RMA-Rae-1β cells (gift of Dr. D. Raulet, Berkeley) was maintained in RPMI 1640 supplemented with 10% FCS. Eco-phoenix cells (Orbigen) were maintained in DMEM supplemented with 10% fetal bovine serum.

DNA construction, transfection, and transduction. cDNA encoding full-length human MICB (allele 0101; ref. 28) was kindly provided by Dr. A. Steinle (University of Tubingen) and subcloned into the retroviral vector pBMNZ-IRES-GFP (Orbigen). To generate recombinant soluble MICB (rsMICB), cDNA encoding the extracellular domain of MICB was amplified by PCR. To generate a putative shedding-resistant form of MICB (designated as MICB.A2), amino acids 215 to 274 of MICB were replaced with the comparable sequence of the α3 domain of HLA-A2 using recombinant PCR of the cDNA sequences (29). rsMICB-FLAG fusion peptide was generated by tagging the cDNA sequence of FLAG (DKYDDDK) to the 3′-end of the rsMICB cDNA using PCR. Error-free amplified cDNAs were identified by sequencing and subcloned into the retroviral vector pBMNZ-IRES-GFP (Orbigen). Plasmids were transfected into Eco-phoenix packaging cells to generate retrovirus. TC2 cells were transduced with respective retrovirus. Stable GFP-positive cell population was isolated by drug selection and sorted by flow cytometry.

Affinity purification of rsMICB and rsMICB-FLAG peptides. The HiTrip NHS-activated column (GE Healthcare) was conjugated with the monoclonal antibody (mAb) 6D4.6 (Santa Cruz Biotechnology) before loading with conditioned medium from TC2-rsMICB or TC2-rsMICB-FLAG cells. After washing, rsMICB or rsMICB-FLAG was eluted with 100 mmol/L sodium citrate (pH 2.5) and neutralized immediately with 1.5 mol/L Tris (pH 8.8).

Immunoprecipitation and Western blotting. Supernatant was collected from TC2-MICB cell culture and passed through a 0.45 μm filter to remove cell debris. Cells were washed and lysed with lysis buffer [50 mmol/L HEPES (pH 7.5), 150 mmol/L NaCl, 1.5 mmol/L $MgCl_2$, 1 mmol/L EGTA, 1% Triton X-100]. Clear supernatant and lysates were incubated with the mAb 6D4.6. Immunocomplexes were collected using protein A/G-agarose (Pierce). PNGase F (New England Biolabs) treatment was carried overnight at 37°C. Immunocomplexes were separated on a 4% to 15% SDS-PAGE, blotted onto a nitrocellulose membrane, and probed with goat anti-MICB antibody AF1599 (R&D Systems). Immunoreactive proteins were detected by incubating the blot with a horseradish peroxidase-conjugated secondary antibody (Pharmacia) and enhanced chemiluminescence reagents (Pharmacia).

MICB shedding assay and (s)MICB ELISA. Cells were seeded at the density of 4×10^5 per well in a 6-well plate in complete medium overnight and replaced with 1 mL/well serum-free medium for 6 h. Supernatant was collected and filtered through 0.45 μm filter. Cells were lysed with 1 mL lysis buffer. Amount of soluble MICB in the supernatant and MICB in the cell lysates was measured using human MICB DuoSet sandwich ELISA kit (R&D Systems). For measuring mouse serum levels of soluble MICB, serum was diluted 1:2 with PBS for ELISA assay.

In vivo *study.* Animal studies were approved by the Institutional Animal Care and Use Committee. Six to 10 severe combined immunodeficient (SCID) male mice (6-week old Harlan-Sprague-Dawley) were used in each group. The following cells (1×10^6 per mouse) were subcutaneously injected into respective group of animals: TC2, TC2-MICB, TC2-MICB.A2, and TC2-rsMICB. All animals were monitored for tumor growth for up to 12 weeks. Tumor volume was estimated using the formula: $V = L \times W^2 / 2$. Animals were euthanized when tumor volumes reached 1,000 mm^3. Tumors, spleens, and peripheral blood were terminally collected. Serum was separated by centrifugation and used for rsMICB ELISA.

In vivo *NKG2D blocking or neutralization.* To block NKG2D receptor, 100 μg of the functional grade of anti-NKG2D blocking antibody CX5 (eBiosciences) were injected intraperitoneally on the day before and the day after tumor implantation and thereafter every 3 days. Blocking was confirmed by flow cytometry of peripheral lymphocytes collected from orbital sinus bleeding with PE-conjugated CX5 (eBiosciences). To modify NKG2D function, animals were injected intraperitoneally with 50 ng purified rsMICB before implantation of TC2-MICB.A2 cells and thereafter twice a week for 4 weeks. Blood was collected once a week from sinus orbital bleeding and serum levels of rsMICB were measured by ELISA.

Flow cytometry. For detection of cell surface expression of NKG2D ligands, TC2 and its derivative cells were trypsinized, blocked with anti-mouse CD16/CD32 (eBiosciences), and incubated with anti-MICA/B mAb 6D4.6 or anti-MICB MAB1599 (R&D Systems) or anti-pan-RAE-1 mAb17582 (R&D Systems) followed by a PE-conjugated secondary

DOI:10.1158/1078-0432.CCR-08-1305

reagent. For detection of rsMICB expression, the BD Cytofix/Cytoperm kit (BD Sciences) was used. Briefly, TC2-rsMICB cells were cultured in the presence of BD GolgiPlug for 3 h to prevent the secretion of rsMICB before harvesting. Cells were resuspended in BD fixation/permeabilization solution for 20 min at 4°C and incubated with 6D4.6 followed with PE-conjugated secondary reagents. For mouse NKG2D binding assay, cells were incubated with 10 μg/mL of the fusion protein of recombinant soluble mouse NKG2D and human Fc (smNKG2D-Fc; R&D Systems) followed by PE-conjugated $F(ab')_2$ goat anti-human IgG. For H-$2K^b$ expression, cells were incubated with $Alex^{647}$-conjugated anti-H-$2K^b/D^b$ mAb (Biolegend).

Single-cell suspensions of splenocytes were prepared as described (30). Cells were stained with FITC-conjugated mAb DX5 (eBiosciences) and PE-conjugated anti-mouse NKG2D mAb CX5 (eBiosciences) or A10 (eBiosciences) and analyzed using a BD FACScan or LSRII. For *ex vivo* rsMICB competitive binding assay, freshly isolated splenocytes were incubated with 10 ng/μL rsMICB-FLAG followed with FITC-conjugated mAb M2 (Sigma-Aldrich) and PE-conjugated mAb DX5 (eBiosciences). Data were analyzed using the BD $CellQuest^{Pro}$ (BD Biosciences) or FlowJo software (Tree Star).

Cytotoxicity assay. Fresh NK cells were prepared using $Spin^{sep}$ murine NK enrichment cocktail (Stem Cell Technology) and were >90% $DX5^+$. LAK cells were prepared by culturing NK cells for 4 to 7 days in 1,000 units/mL recombinant human interleukin-2. Cytotoxicity was done in triplicates using the standard 4 h ^{51}Cr release assay (13). Antibody blocking was done by preincubating effector cells with 30 μg/mL NKG2D blocking mAb CX5 (eBiosciences) or preincubating target cells with 100 μg/mL anti-pan RAE-1 polyclonal antibody at 37°C for 1 h (31).

Statistical analysis. Data were analyzed using JMP software. Significance between two animal groups was determined by Student's *t* test. $P < 0.05$ was considered significant.

Results

Putative cleavage region of MIC(B) in TC2 tumor cells. TC2 is a mouse prostate tumor cell line generated from the TRAMP mouse (27), which does not express any homologous molecules to human MIC (28). TC2 cells were transduced with retroviruses that carry cDNAs of human MICB and GFP. Transduced cells stably expressing high levels of MICB (designated as TC2-MICB cells) were generated by puromycin selection and multiple rounds of flow cytometry cell sorting for GFP-positive cells.

To generate a shedding-resistant form of MICB, we first performed experiments to predict putative cleavage region of MICB by tumor cells. Soluble MICB resulted from TC2 shedding (designated as ssMICB) was immunoprecipitated from supernatant of TC2-MICB cells with a mouse mAb 6D4.6 specific to the α1α2 ectodomain of MICA/B (10). The full-length MICB was immunoprecipitated from cell lysates with the same antibody. Immunocomplexes were separated and immunoblotted with a goat polyclonal antibody AF1599 specific to the ectodomain of MICB. After N-glycosidase (PNGase F) treatment, ssMICB yield two bands of molecular mass ~31 to 33 kDa (Fig. 1A). The molecular mass is consistent with other studies showing soluble MICB and soluble MICA released by human tumor cells (32, 33). When samples were treated with dinitrothiocyanobenzene, a disulfide isomerase inhibitor, only a single band of soluble MICB was revealed (data not shown), suggesting that the two bands of soluble MICB released by TC2 cells are the reduced and nonreduced forms of ssMICB. Similar observation of soluble MICA shed by human tumor cell lines was shown by Kaiser et al. (33). The deglycosylated full-length MICB is shown to be ~41 kDa in the cell lysates (Fig. 1A), consistent with other studies (34). Although the precise cleavage site cannot be determined, these data suggest that MICB was cleaved at the α3 domain proximal to the transmembrane region to generate ssMICB (Fig. 1B). Similar cleavage region is also predicted for human tumor cell lines to generate soluble MICA (33).

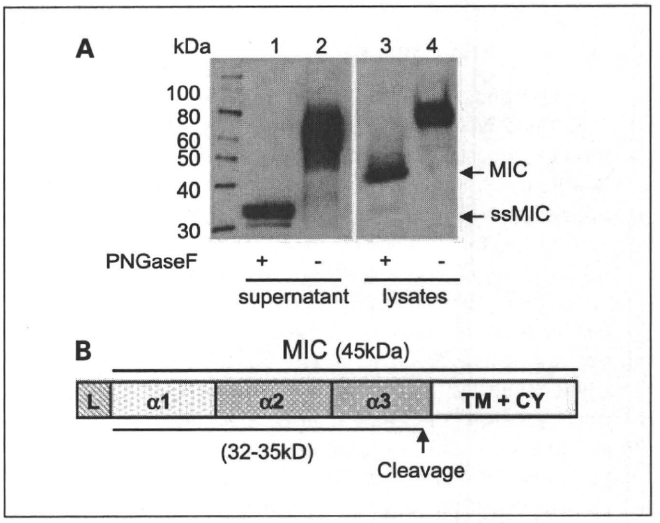

Fig. 1. Putative MICB cleaved site(s) in TC2 cells. *A*, Western blot showing the predicted size of cleaved soluble MICB in TC2 cells. Supernatant and lysates of TC2-MICB cells were immunoprecipitated with anti-MIC mAb 6D4.6. The immunocomplexes were treated with PNGase F and resolved on SDS-PAGE. Proteins were transferred to nitrocellulose membrane and blotted with goat anti-MICB polyclonal antibody. *Lanes 1* and *2*, detection of soluble MICB from TC2-MICB supernatant. The molecular mass of the deglycosylated cleaved soluble MICB is estimated to be 31 to 33 kDa. *Lanes 3* and *4*, detection of full-length MICB from TC2-MICB cell lysates. The full-length deglycosylated MICB is estimated to be 41 kDa on 4% to 15% SDS-PAGE. *B*, putative MICB cleavage site(s).

Generation of tumor cell lines expressing the putative shedding-resistant MICB.A2 and rsMICB. To study the effect of MIC shedding on tumor formation and growth *in vivo*, we generated two forms of MICB, the recombinant secretable form of MICB (rsMICB) and a putative shedding-resistant form of MICB (MICB.A2). rsMICB was generated by deletion of the transmembrane and cytoplasmic domains. MICB.A2 was generated by replacing part of the α3 domain of MICB (amino acids 215-274) with the corresponding residues from HLA-A2 (Fig. 2A). Because NKG2D only interacts with the α1α2 domain of MIC (24), MICB.A2 would presumably continue to recognize NKG2D. rsMICB and MICB.A2 were overexpressed in TC2 cells using the GFP retroviral system described above. Positive-expressing clones were selected by puromycin and repeated sorting by flow cytometry for GFP-positive cells. The expression level of cellular rsMICB and surface MICB.A2 in TC2 cells was confirmed by flow cytometry with the anti-MIC mAb 6D4.6 (Fig. 2B).

Partial replacing the α3 domain of MICB protects from tumor cell shedding. An ELISA assay was used to assess the degree of shedding of MICB and MICB.A2 in TC2 cell lines. Both the capture and the detection antibodies are specific to the extracellular domain of MICB and can also detect MICB.A2 by Western blotting (data not shown). With a given number of cells, the amount of cleaved soluble MIC in the culture supernatant and the amount of MIC in the lysates were

DOI:10.1158/1078-0432.CCR-08-1305

measured by a sandwich ELISA assay (Fig. 2C). The degree of MIC shedding was estimated by the molar percentage of soluble MICB released into the supernatant. Approximately 30% of MICB was cleaved into the medium in TC2 cells, whereas no cleaved form of MICB.A2 was detectable in the culture supernatant (Fig. 2C). This indicates that MICB.A2 cannot be cleaved into soluble forms by tumor cells and is shedding-resistant.

Expression of MICB.A2 in TC2 cells stimulates mouse NK cell cytolytic activity. Human MICB can be recognized by mouse NKG2D and activate mouse NK cells (22, 23). To test whether overexpressing MICB.A2 can also activate mouse NK cells, we first addressed the physical interaction of MICB.A2 with soluble mouse NKG2D-Fc (smNKG2D-Fc) fusion protein by flow cytometry analyses. As measured by mean fluorescence intensity (Fig. 3A), smNKG2D-Fc was more prominently bound by TC2-MICB and TC2-MICB.A2 cells and only weakly bound by TC2 and TC2-rsMICB cells. Accordingly, *in vitro* cytotoxicity assay revealed marked increase in sensitivity of TC2 cells to interleukin-2-activated mouse NK (LAK) cells when MICB or MICB.A2 was overexpressed (Fig. 3B; $P < 0.01$). The increased susceptibility of TC2-MICB and TC2-MICB.A2 cells to LAK cells can be inhibited by preincubation of LAK cells with the NKG2D-specific blocking antibody CX5 (ref. 35; Fig. 3B), suggesting a NKG2D-dependent LAK cell-killing effect. Thus, the shedding-resistant MICB.A2 maintained the functional property of MICB to be recognized by mouse NKG2D.

Although not expressing any MIC homologue, TC2 cells express some levels of endogenous NKG2D ligand RAE-1 variants but not H60 (22, 36). However, the level of endogenous NKG2D ligands is not sufficient to stimulate LAK cell *in vitro* cytotoxicity (Fig. 3B). To address whether the increased

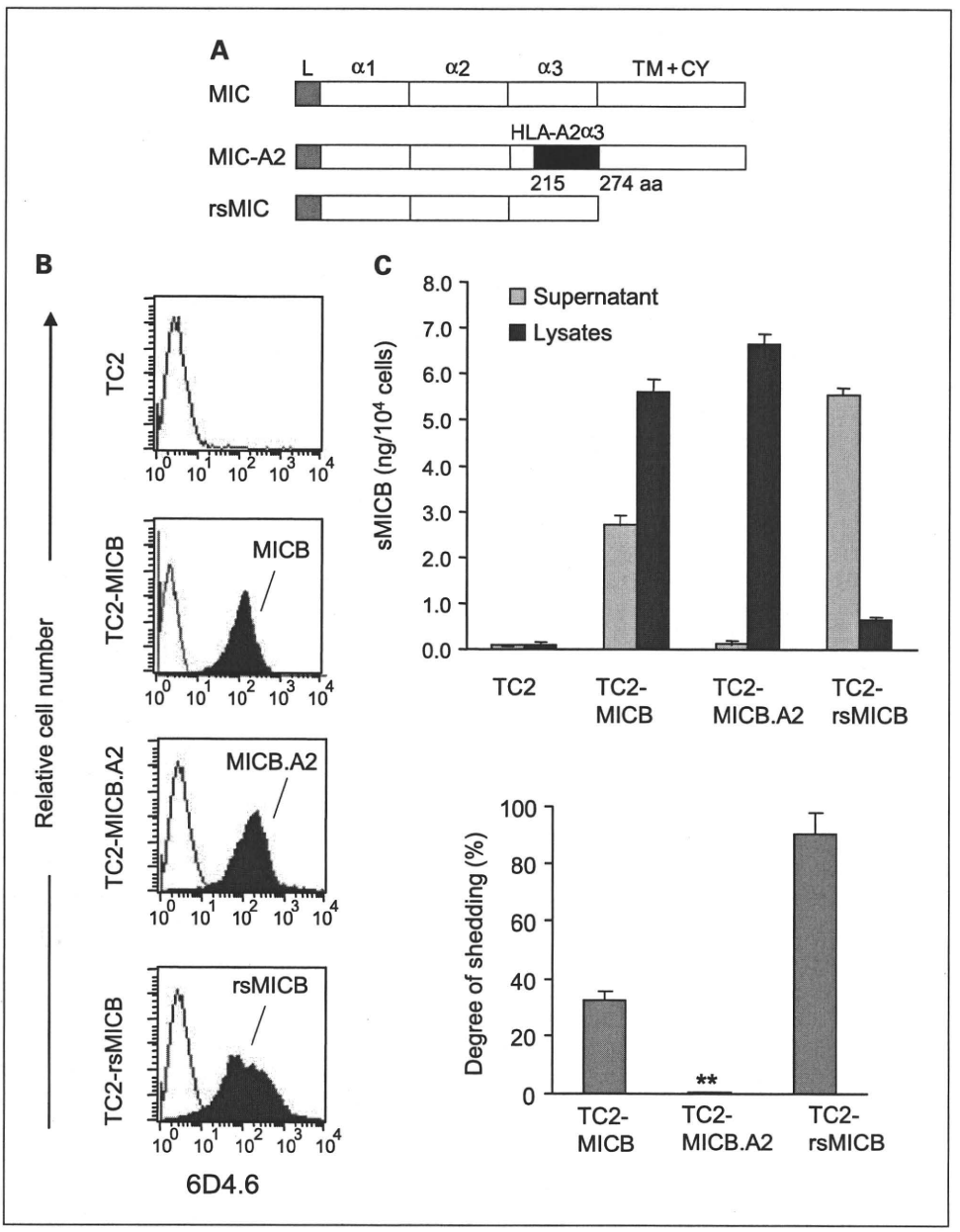

Fig. 2. Construction and expression of the shedding-resistant noncleavable and soluble recombinant forms of MICB (rsMICB) in TC2 cell lines. *A,* generation of the noncleavable form MICB.A2 by replacing amino acids 215 to 274 of the MICB α3 domain with the corresponding sequence of HLA-A2. rsMICB was generated by deletion of the entire transmembrane and cytoplasmic region of MICB. *B,* flow cytometry showing expression levels of MICB, MICB.A2, and rsMICB in TC2 cell lines. cDNAs of MICB, MICB.A2, or rsMICB were inserted into a IRES-GFP retroviral vector pBMNZ. TC2 cells were transduced with respective retrovirus. GFP-positive cells were sorted by flow cytometry. For detection of MICB and MICB.A2 expression, cells were directly incubated with anti-MIC 6D4.6 antibody followed a PE-conjugated secondary reagent. For detection of the secretable rsMICB expression, TC2-rsMICB cells were cultured in the presence of BD GolgiPlug for 3 h to prevent the secretion of rsMICB before harvesting. Cells were resuspended in BD Fixation/Permeabilization solution for 20 min at 4°C and incubated with 6D4.6 followed with a PE-conjugated secondary reagent. *C,* MICB.A2 is shedding-resistant. *Top,* amount of shed soluble MICB in the culture supernatant and MICB in the cell lysates. Cells (4×10^5 per well) were plated on a 6-well plate overnight. Medium was removed and replaced with 1 mL serum-free medium. Six hours later, medium was collected and filtered. Cells were lysed with 1 mL lysis buffer, and 50 μL culture supernatant and cell lysates were used for (s) MICB ELISA assay. *Bars,* SE. *Bottom,* degree of shedding as calculated by molars of soluble MICB in the supernatant versus total molars of soluble MICB and MICB (a sum of supernatant and cell lysates). Final results were normalized by cell numbers at the time of the assay. Results of three independent experiments. *, $P < 0.001$.

DOI:10.1158/1078-0432.CCR-08-1305

sensitivity of TC2-MICB and TC2-MICB.A2 cells to LAK cell killing is possibly due to increased expression of RAE-1, we analyzed endogenous RAE-1 expression on these cell lines by flow cytometry with a rat anti-pan RAE-1 mAb. A consistency of RAE-1 expression among TC2, TC2-MICB, and TC2-MICB.A2 cell lines is shown in Fig. 3C. Furthermore, preincubation of target cells with an anti-pan RAE-1 blocking antibody (30) did not significantly reduce the susceptibility of TC2-MICB or TC2-MICB.A2 cells to LAK cells, whereas the sensitivity of the control RMA-Rae-1β cells to LAK cells was significantly reduced (Fig. 3B). These suggest that the increased killing of TC2-MICB or TC2-MICB.A2 cells by LAK cells is not due to increased RAE-1 expression.

TC2 cells express a very low level of H-2K^b/D^b (37), which is a potential ligand for inhibitory Ly49 receptor families. We analyzed H-2K^b/D^b expression on these cell lines by flow cytometry. Consistent levels of H-2K^b/D^b expression were found in TC2 and cell lines expressing MICB or MICB.A2 (Fig. 3C), suggesting that the increased sensitivity of TC2-MICB and TC2-MICB.A2 cells to LAK cells was not attributed to a reduced level of H-2K^b/D^b expression.

***Shedding-resistant MICB.A2 but not the natural MICB prevents TC2 tumor formation* in vivo.** In three independent experiments, when SCID animals were implanted with TC2-rsMICB, TC2-MICB, or TC2-MICB.A2 cells, none of animals that were implanted with the TC2-MICB.A2 cells developed tumors with a 12-week follow-up observation period, whereas all the animals that were implanted with TC2-rsMICB or TC2-MICB cells developed tumors within 3 weeks (Fig. 4A and B). In addition, no significant difference in tumor growth was observed among TC2, TC2-rsMICB, and TC2-MICB originated tumors (Fig. 4A). To address whether the failure to reject TC2-MICB tumors is due to the large dose (1×10^6) of tumor cells injected, we repeated the experiment with TC2-MICB and TC2-MICB.A2 cells using smaller numbers of inoculated cells. A 10-fold (1×10^5) and a 100-fold (1×10^4) decrease in the number of inoculated tumor cells did not change the outcome (Fig. 4C). We also examined MICB expression in the TC2-MICB-originated tumor cells extracted from SCID animals by flow cytometry. All the extracted tumor cells expressed the similar levels of MICB before implantation (Fig. 4D). This suggests that tumor growth in animals that were implanted with TC2-MICB cells is not due to NK cells selectively eliminating MICB-positive cells.

Shedding of MICB by TC2 cells allows TC2-MICB tumor growth in mice. In 4 h *in vitro* cytotoxicity assays, both TC2-MICB and TC2-MICB.A2 cells were sensitive to LAK cells (Fig. 3B). However, NK tumor immunity was effective only in animals when the noncleavable MICB.A2 was expressed on tumor cells. We propose that the discrepancy of *in vivo* and *in vitro* observation is attributed to tumor cell shedding of MICB *in vivo*, which accumulatively compromises NK cell function in animals implanted with MICB-expressing tumor cells. To test this hypothesis, we measured serum levels of soluble MICB in all the animals 4 weeks after tumor implantation using a sandwich ELISA assay. A significant level of soluble MICB was detected in the sera of animals that were implanted with tumor cells expressing rsMICB and MICB, whereas no soluble MICB was detectable in animals implanted with tumor cells expressing MICB.A2 (Fig. 5A). To address why TC2-MICB cells were sensitive to LAK cell *in vitro*, LAK cells were incubated with the supernatant of TC2-MICB cells for various periods and used as

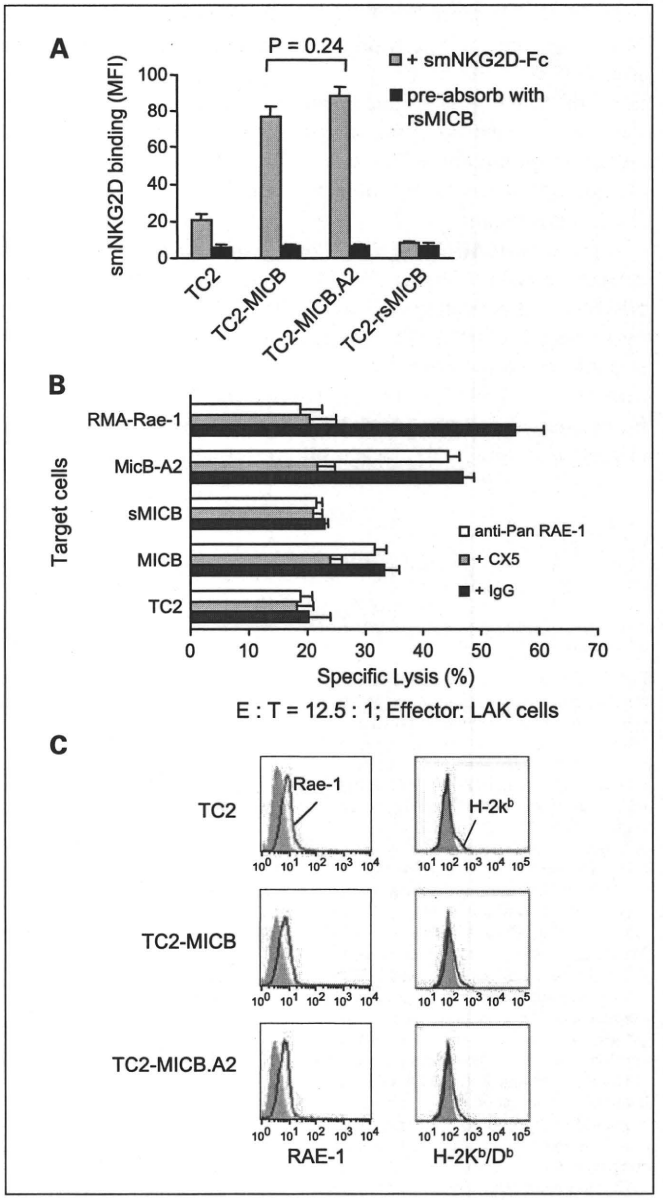

Fig. 3. Overexpression of MICB and MICB.A2 increases the sensitivity of TC2 cells to NK cell killing. *A,* binding of MICB and MICB.A2 by mouse NKG2D. Cells were incubated with the chimeric soluble mouse NKG2D-human Fc (smNKG2D-Fc) followed by PE-conjugated anti-human IgG. Cells were analyzed by flow cytometry. Data are mean fluorescence intensity. When smNKG2D-Fc was preabsorbed with rsMICB, no binding was seen in any of the cell lines. No significant difference was shown in the binding ability between MICB and MICB.A2 ($P = 0.24$). *B,* sensitivity of various MICB-expressing TC2 cells to mouse NK cells. NK cells were isolated from SCID mice and cultured in complete medium with 1,000 units/mL interleukin-2 for 4 d before used as effectors in standard 4 h ^{51}Cr release assay. For blocking NKG2D receptor, effector cells were preincubated with 30 μg/mL CX5 antibody. For blocking RAE-1, target cells were preincubated with 100 μg/mL anti-pan-RAE-1 polyclonal antibody for 1 h before the assay. RMA-Rae-1 βcells were used as positive controls for blocking antibodies. *E:T,* effector:target ratio. *Bars,* SE. *, $P < 0.01$, compared with TC2 cells as targets. *C,* flow cytometry histograms showing surface expression of RAE-1 (*left*) and H-2K^b/D^b (*right*) in TC2, TC2-MICB, and TC2-MICB.A2 cells. *Filled histograms,* cells were stained with control isotype antibodies; *open histograms,* cells were stained with specific antibodies. Results of three independent experiments.

effector cells to kill target TC2-MICB.A2 cells. Only after 8 h incubation, LAK cell-killing ability was significantly affected. Therefore, in the 4 h *in vitro* cytotoxicity assay, the killing ability of LAK cells was not significantly affected by soluble MICB

DOI:10.1158/1078-0432.CCR-08-1305

resulted from target TC2-MICB cells (data not shown). We further examined NK cell tumor-killing ability from these animals. For this purpose, freshly isolated splenic NK cells were used as effector cells for *in vitro* cytotoxicity assay. NK cells from mice bearing MICB- and rsMICB-expressing tumors had a significant reduction in cytotoxicity against TC2-MICB.A2 target cells in comparison with those from TC2 tumor-bearing or tumor-free animals ($P < 0.01$; Fig. 5B). The cytotoxicity of these NK cells was inhibited by preincubating with a NKG2D-specific inhibitory mAb CX5 (Fig. 5B), suggesting a NKG2D-dependent effect. Together, these results suggest that persistent presence of soluble MICB *in vivo* due to tumor cell shedding of MICB compromised NKG2D-mediated NK cell lytic activity and thus permitted the growth of MICB-expressing tumor cells.

Persistent presence of soluble MICB blocks the NKG2D-mediated NK cell recognition of target cells. When animals were treated with the CX5 antibody to block NKG2D receptor, injection of TC2-MICB.A2 cells gave rise to tumor formation in all the SCID animals (Fig. 6A). This suggests that the inhibition of TC2-MICB.A2 tumor formation in SCID animals is NKG2D-dependent. To test the effect of presence of soluble MICB on tumor formation of MICB.A2-expressing cells, we injected animals with purified rsMICB (50 ng) before and after implanting TC2-MICB.A2 cells. Under this experimental

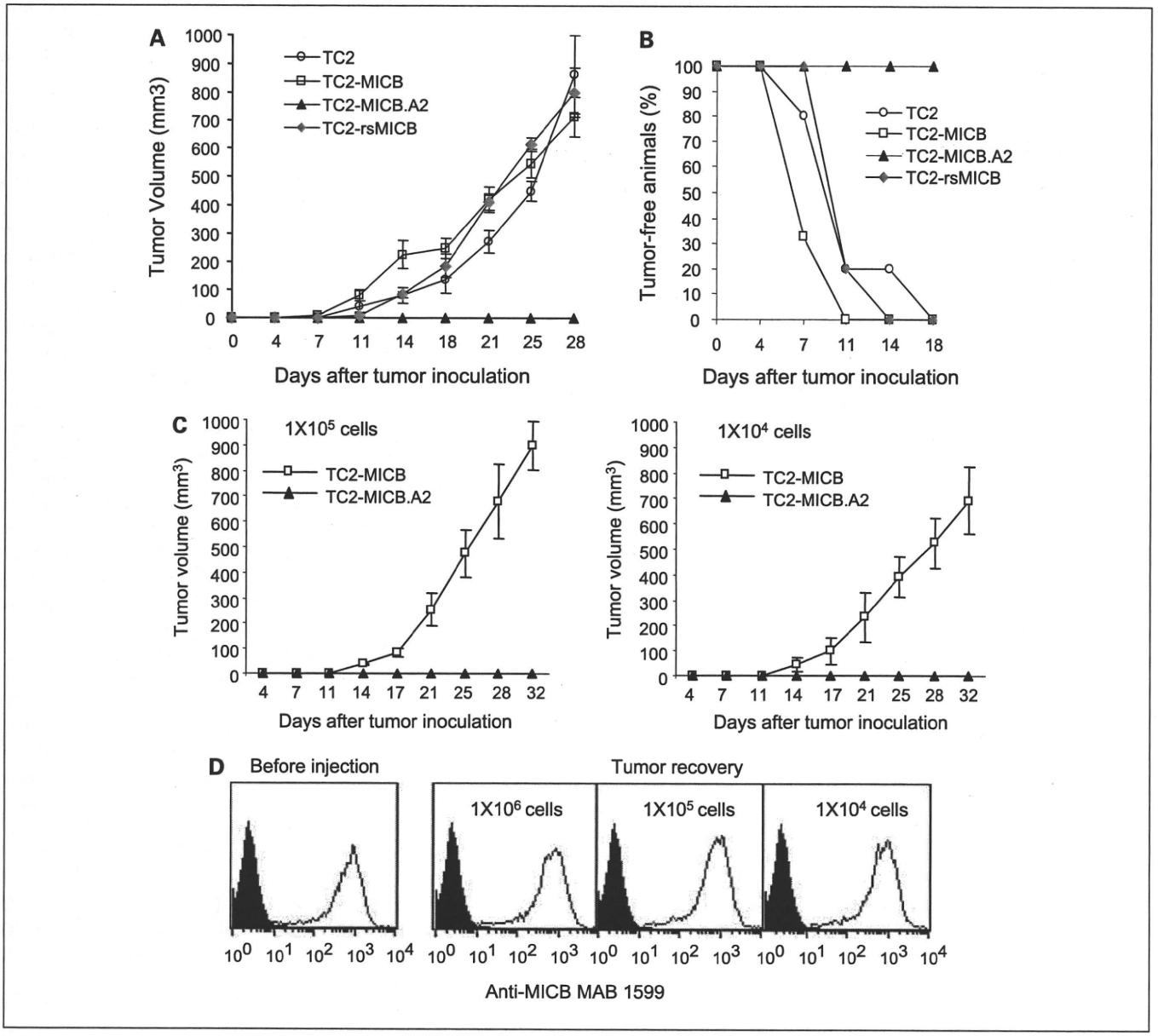

Fig. 4. Expression of MICB.A2 but not the cleavable MICB prevents tumor formation *in vivo*. Six animals were used in each group. Tumor growth was monitored twice weekly. Tumor volume was estimated by the formula: $V = L^2 \times W / 2$. *A*, tumor growth of various MICB-expressing TC2 cells in SCID mice. *B*, rate of tumor formation of various MICB-expressing TC2 cells in SCID mice. Cells (1×10^6) were injected subcutaneously into each animal in *A* and *B*. *C*, tumor growth of TC2-MICB cells when injected at lower doses (1×10^5 and 1×10^4 cells per animal). *D*, representative flow cytometry histoplots showing MICB expression in tumor cells extracted from animals inoculated with TC2-MICB cells compared with prior inoculation. The MICB-specific antibody MAB1599 (R&D Systems) was used as primary antibody. *Filled histogram*, MICB expression in TC2 cells; *open histogram*, MICB expression in TC2-MICB cells or tumor cells. Results of three independent experiments.

DOI:10.1158/1078-0432.CCR-08-1305

condition, implantation of TC2-MICB.A2 cells gave 100% tumor formation (Fig. 6A). Tumor cells extracted from these animals were shown to be GFP-positive and express MICB.A2 by flow cytometry analyses (data not shown). NK cells isolated from these animals showed very little cytolytic activity against TC2-MICB.A2 target cells (data not shown). These data suggest that persistent presence of soluble MICB compromises the cytotoxicity of NK cells against TC2-MICB.A2 cells.

We sought the mechanisms by which tumor shedding-derived soluble MICB would diminish NK cell activity. Soluble MICB may down-modulate surface NKG2D expression on NK cells (16) or block the recognition of NK cells to target cells by physical occupancy of the NKG2D receptor. To distinguish these two mechanisms, we first analyzed NKG2D expression on splenic NK cells freshly isolated from animals injected with various TC2 tumor cells using flow cytometry analyses with a nonblocking NKG2D antibody A10 (29). There was no significant difference in surface NKG2D expression on NK cells from mice bearing TC2-MICB and TC2-rsMICB tumors compared with those from animals bearing TC2 tumors or tumor-free animals (Fig. 6B), suggesting that the suppressive effect of soluble MICB on NK cell activity was not through down-modulation of surface NKG2D receptor. We further examined the occupancy of NKG2D receptor on NK cells by tumor-derived soluble MICB using competitive binding assay. Freshly isolated splenocytes were incubated with purified rsMICB-FLAG, and NK cell-binding ability to rsMICB-FLAG was measured by flow cytometry using the anti-FLAG mAb M2.

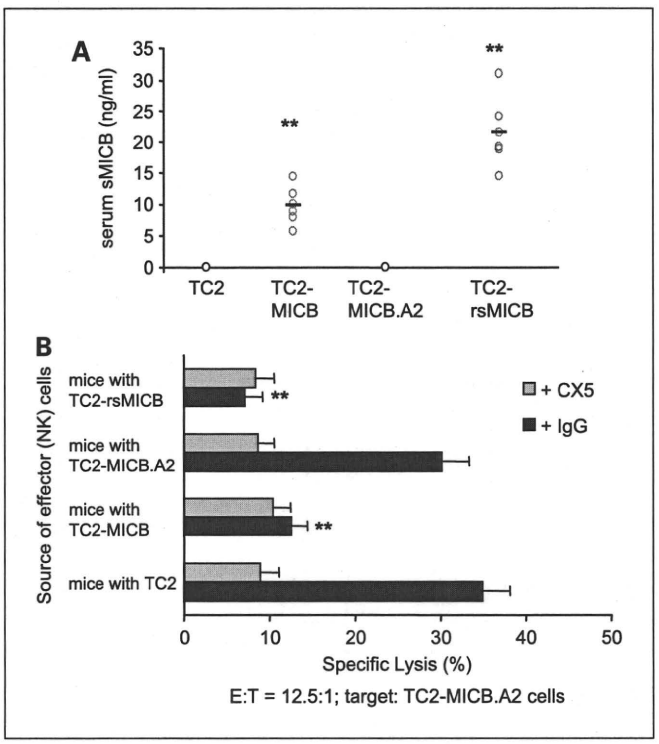

Fig. 5. Shedding of MICB by TC2-MICB cells compromises NK cell activity *in vivo*. *A*, serum levels of soluble MICB in all the tumor-bearing animals. *B*, reduced NKG2D-dependent NK cell cytotoxicity of splenic NK cells from animals bearing TC2-rsMICB and TC2-MICB tumors. Freshly isolated NK cells were used as effectors; TC2-MICB.A2 cells were used as target cells. **, $P < 0.01$, compared with TC2 or TC2-MICB.A2. Results of three independent experiments.

NK cells from animals inoculated with TC2-MICB or TC2-rsMICB cells had significantly reduced binding to rsMICB-FLAG compared with those from animals inoculated with TC2 or TC2-MICB.A2 cells ($P < 0.01$; Fig. 6C). Together, these data suggest that soluble MICB dampens NKG2D-dependent NK cell activity mainly by masking the NKG2D receptor and thus blocking the interaction of NKG2D with target molecules.

Discussion

This study has provided conclusive evidence supporting the hypothesis that shedding of MIC by transformed cells can promote tumor growth. In this study, we generated a shedding-resistant NKG2D ligand MICB.A2 by partially modifying the α3 domain of MICB and showed that overexpressing MICB.A2 prevented tumor formation by the mouse prostate tumor cell line TC2. We also showed that, when soluble MICB was persistently present, expression of the shedding-resistant MICB.A2 on the tumor cell surface did not prevent or delay tumor formation *in vivo*. Our study signifies the effect of MIC shedding on tumor formation and the magnitude of sustained MIC-induced NKG2D immunity in preventing early tumor development.

Although the mechanisms of MIC shedding is still under investigation (19, 33, 38), clinical evidence has shown that shedding of MIC is common in MIC-positive cancers, such as prostate, colon, breast adenocarcinomas, and melanomas (10–13). In these patients, the function of NK and/or CD8 T cells was compromised due to soluble MIC-induced internalization of the NKG2D receptor (13, 16–18). Thus, it was hypothesized that MIC shedding in tumors can promote tumor immune evasion and progress to advanced disease. Recent studies have shown that MIC expression is not restricted in tumor cells and that MIC can be induced in cells in response to DNA damage (39), a prior event to transformation. Therefore, the current study indicates that, in the event of malignant transformation, inhibiting shedding of MIC from MIC-positive transformed cells can prevent the initiation of tumor formation.

We chose to overexpress human MICB rather than mouse NKG2D ligands in this study for the following rationales. Firstly, MIC has been shown to be shed by tumor cells in cancer patients; thus, the study is clinically relevant. Secondly, MICB has been shown to interact with mouse NKG2D, and MICB-positive cells are sensitive to mouse NK cells (22, 23). We also have shown that MICB was shed by the mouse prostate cell line TC2 in the same pattern as MIC shedding in prostate cancer patients.[4] Thirdly, although mouse NKG2D ligands are functionally similar to human MIC in NK cell activation, these molecules are structurally different and may have different physiologic roles. Mouse NKG2D ligands lack the α3 domain and are mostly GPI-linked proteins (9); in addition, little is known about what controls the expression of mouse NKG2D ligands *in vivo* and whether they would shed in a similar fashion to MIC in human tumor cells. Lastly, different from human NKG2D ligands, studies have shown that naturally expressed mouse NKG2D ligands on tumor cells may not cause tumor rejection largely due to insufficient levels of the ligand expression (2) or low affinity of binding to NKG2D (40). In

[4] Wu, unpublished data.

DOI:10.1158/1078-0432.CCR-08-1305

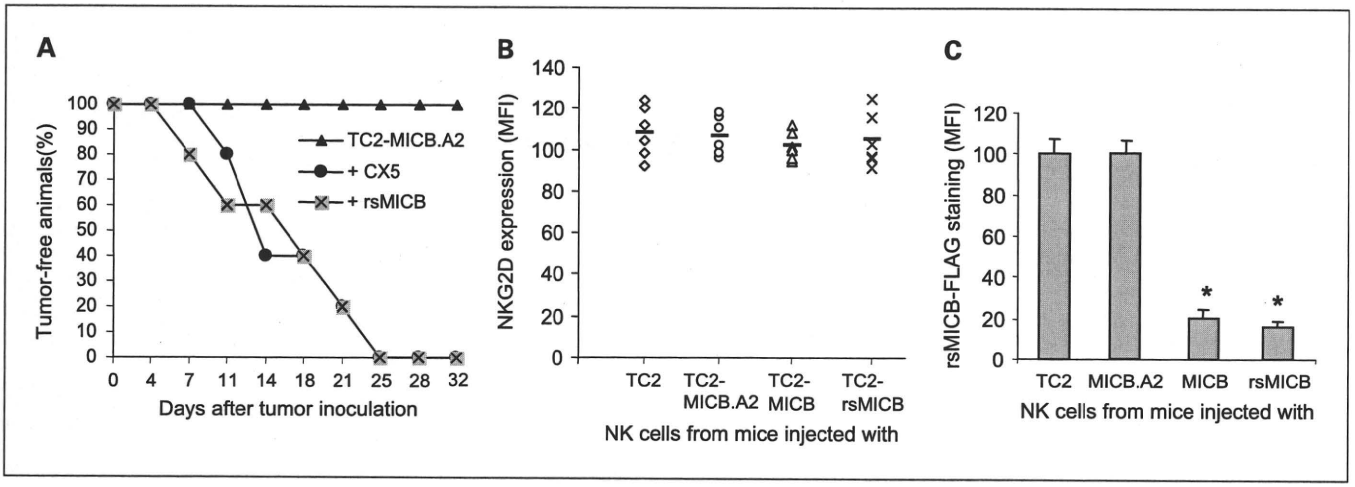

Fig. 6. Soluble MICB-induced NK cell dysfunction. *A, in vivo* blocking NKG2D with CX5 antibody or neutralization the function of NKG2D with rsMICB enables TC2-MICB.A2 cells to form tumors. To block NKG2D receptor *in vivo*, 100 μg NKG2D-specific antibody CX5 was injected intraperitoneally on the day before and the day after tumor implantation and thereafter every 3 d. To modify NKG2D function, animals were intraperitoneally injected with 50 ng purified rsMICB before implantation of TC2-MICB.A2 cells and thereafter twice a week for 4 wk. *B,* measurements of NKG2D expression shown as mean fluorescence intensity on splenic NK cells freshly isolated from SCID animals ($n = 6$) injected with various tumor cells. *Columns,* mean fluorescence intensity. *C,* competitive binding assay indicating saturation of NKG2D receptor by soluble MICB in animals bearing TC2-MICB and TC2-rsMICB tumors. Freshly isolated splenocytes were incubated with 10 ng/μL rsMICB-FLAG followed by FITC-conjugated anti-FLAG mAb M2 and PE-conjugated mAb DX5. Data are measurements of mean fluorescence intensity of M2 staining from six animals of each experimental group. *Bars,* SE. *, $P < 0.01$, compared with animals injected with TC2 or TC2-MICB.A2 tumor cells.

this study, although TC2 cells express some levels of mouse NKG2D ligand RAE-1 variants, TC2 tumors were palpable in SCID mice within 1 week after implantation and grew aggressively (Fig. 4), suggesting that the levels of activating RAE-1 variants expressed by TC2 cells are too low to induce antitumor immunity. This was also supported by the low binding ability of soluble mouse NKG2D to TC2 cells (Fig. 3A). Therefore, it could be challenging to define an optimal level of mouse NKG2D ligand expression for tumor rejection. Together, the choice of MICB makes the *in vivo* study described here more clinically relevant to human cancers.

In activated mouse NK cells, due to alternative DNA splicing, two isoforms of NKG2D couple with two intracellular adaptors, DAP10 and DAP12, which trigger phosphatidylinositol 3-kinase and Syk family protein tyrosine kinase, respectively (40, 41). In human, NKG2D only associates with DAP10. However, in mouse NK cells lacking DAP12 or Syk family kinases, DAP10-phosphatidylinositol 3-kinase pathway alone is sufficient to initiate ligand-induced NKG2D-mediated killing of target cells (41). Thus, regardless that signaling via mouse NKG2D is more complex than human NKG2D, effect of NKG2D ligand shedding on tumor formation as found in the current study would be significant in both species.

Most of the *in vitro* evidence suggests that engagement of tumor cell surface MIC to NKG2D can activate NK cell immunity against tumor cells. Thus, expression of MIC on tumor cells is proposed to activate host protective antitumor immunoresponse. However, most of the epithelial originated human cancer cells were found to have MIC expressed on the surface, suggesting the ineptness of MIC-induced NK cell immunity. Consistent with clinical observations, we also show that overexpressing the natural cleavable form of MICB in TC2 cells has no significant effect on tumor growth *in vivo*. Although overexpressing the noncleavable shedding-resistant MICB.A2 can cause TC2 tumor rejection, this effect can be inhibited by the persistent presence of soluble MICB (Fig. 6A). Together, our data suggest that the role of MIC in host tumor immunosurveillance is determined by whether MIC is all or partially membrane-bound. If all the MIC molecules sustain to be membrane-bound and noncleavable, expression of MIC activates NK cell-mediated host immunity. In contrast, if a portion of the MIC molecules is cleaved and becomes soluble, tumor cells cannot be targeted by NK cells due to soluble MIC-mediated masking and possible down-regulation of the receptor NKG2D regardless of abundant MIC remaining on the tumor cell surface as observed in many cancer patients (10–13).

In summary, our data provide the first *in vivo* conclusive evidence of the effect of MIC shedding on tumor growth and the importance of sustained MIC ligand-NKG2D receptor interaction in control of tumor growth. In addition, our results show no significant difference in tumor growth among animals whether the natural form of MICB or soluble recombinant MICB was expressed. This observation implies that wild-type MIC expression in established tumors may have very little effect on inducing host NK cell activation due to shedding of MIC by tumor cells and the consequent dampening of host immunity. Together, our results suggest that strategies to sustain the recognition of NKG2D receptor and tumor MIC ligand may have potential anticancer therapeutic implications.

Disclosure of Potential Conflicts of Interest

No potential conflicts of interest were disclosed.

Acknowledgments

We thank Michael Tao for assistance with animal tissue collections and Dr. Norman M. Greenberg for helpful discussions.

DOI:10.1158/1078-0432.CCR-08-1305

References

1. Cerwenka A, Bakker AB, McClanahan T, et al. Retinoic acid early inducible genes define a ligand family for the activating NKG2D receptor in mice. Immunity 2000; 12:721–7.
2. Diefenbach A, Jensen ER, Jamieson AM, Raulet DH. Rae1 and H60 ligands of the NKG2D receptor stimulate tumour immunity. Nature 2001;413:165–71.
3. Cerwenka A, Baron JL, Lanier LL. Ectopic expression of retinoic acid early inducible-1 gene (RAE-1) permits natural killer cell-mediated rejection of a MHC class I-bearing tumor *in vivo*. Proc Natl Acad Sci U S A 2001; 98:11521–6.
4. Diefenbach A, Hsia JK, Hsiung MY, Raulet DH. A novel ligand for the NKG2D receptor activates NK cells and macrophages and induces tumor immunity. Eur J Immunol 2003;33:381–91.
5. Carayannopoulos LN, Naidenko OV, Fremont DH, Yokoyama WM. Cutting edge: murine UL16-binding protein-like transcript 1: a newly described transcript encoding a high-affinity ligand for murine NKG2D. J Immunol 2002;169:4079–83.
6. Smyth MJ, Swann J, Cretney E, Zerafa N, Yokoyama WM, Hayakawa Y. NKG2D function protects the host from tumor initiation. J Exp Med 2005;202:583–8.
7. Long EO. Tumor cell recognition by natural killer cells. Semin Cancer Biol 2002;12:57–61.
8. Raulet DH. Roles of the NKG2D immunoreceptor and its ligands. Nat Rev Immunol 2003;3:781–90.
9. Cerwenka A, Lanier LL. NKG2D ligands: unconventional MHC class I-like-molecules exploited by viruses and cancer. Tissue Antigens 2003;61:335–43.
10. Groh V, Rhinehart R, Secrist H, Bauer S, Grabstein KH, Spies T. Broad tumor-associated expression and recognition by tumor-derived γδ T cells of MICA and MICB. Proc Natl Acad Sci U S A 1999;96:6879–84.
11. Vetter CS, Groh V, thor Straten P, Spies T, Brocker EB, Becker JC. Expression of stress-induced MHC class I related chain molecules on human melanoma. J Invest Dermatol 2002;118:600–5.
12. Jinushi M, Takehara T, Tatsumi T, et al. Expression and role of MICA and MICB in human hepatocellular carcinomas and their regulation by retinoic acid. Int J Cancer 2003;104:354–61.
13. Wu JD, Higgins LM, Steinle A, Cosman D, Haugk K, Plymate SR. Prevalent expression of the immunostimulatory MHC class I chain-related molecule is counteracted by shedding in prostate cancer. J Clin Invest 2004;114:560–8.
14. Friese MA, Platten M, Lutz SZ, et al. MICA/NKG2D-mediated immunogene therapy of experimental gliomas. Cancer Res 2003;63:8996–9006.
15. Busche A, Goldmann T, Naumann U, Steinle A, Brandau S. Natural killer cell-mediated rejection of experimental human lung cancer by genetic overexpression of major histocompatibility complex class I chain-related gene A. Hum Gene Ther 2006;17: 135–46.
16. Groh V, Wu J, Yee C, Spies T. Tumour-derived soluble MIC ligands impair expression of NKG2D and T-cell activation. Nature 2002;419:734–8.
17. Doubrovina ES, Doubrovin MM, Vider E, et al. Evasion from NK cell immunity by MHC class I chain-related molecules expressing colon adenocarcinoma. J Immunol 2003;171:6891–9.
18. Raffaghello L, Prigione I, Airoldi I, et al. Downregulation and/or release of NKG2D ligands as immune evasion strategy of human neuroblastoma. Neoplasia 2004;6:558–68.
19. Salih HR, Rammensee HG, Steinle A. Cutting edge: down-regulation of MICA on human tumors by proteolytic shedding. J Immunol 2002;169: 4098–102.
20. Holdenrieder S, Stieber P, Peterfi A, Nagel D, Steinle A, Salih HR. Soluble MICA in malignant diseases. Int J Cancer 2006;118:684–7.
21. Marten A, von Lilienfeld-Toal M, Buchler MW, Schmidt J. Soluble MIC is elevated in the serum of patients with pancreatic carcinoma diminishing γδ T cell cytotoxicity. Int J Cancer 2006;119:2359–65.
22. Diefenbach A, Jamieson AM, Liu SD, Shastri N, Raulet DH. Ligands for the murine NKG2D receptor: expression by tumor cells and activation of NK cells and macrophages. Nat Immunol 2000;1:119–26.
23. Dunn C, Chalupny NJ, Sutherland CL, et al. Human cytomegalovirus glycoprotein UL16 causes intracellular sequestration of NKG2D ligands, protecting against natural killer cell cytotoxicity. J Exp Med 2003;197:1427–39.
24. Li P, Morris DL, Willcox BE, Steinle A, Spies T, Strong RK. Complex structure of the activating immunoreceptor NKG2D and its MHC class I-like ligand MICA. Nat Immunol 2001;2:443–51.
25. Holmes MA, Li P, Petersdorf EW, Strong RK. Structural studies of allelic diversity of the MHC class I homolog MIC-B, a stress-inducible ligand for the activating immunoreceptor NKG2D. J Immunol 2002; 169:1395–400.
26. Strong RK. Asymmetric ligand recognition by the activating natural killer cell receptor NKG2D, a symmetric homodimer. Mol Immunol 2002;38: 1029–37.
27. Foster BA, Gingrich JR, Kwon ED, Madias C, Greenberg NM. Characterization of prostatic epithelial cell lines derived from transgenic adenocarcinoma of the mouse prostate (TRAMP) model. Cancer Res 1997;57:3325–30.
28. Bahram S, Spies T. Nucleotide sequence of a human MHC class I MICB cDNA. Immunogenetics 1996;43: 230–3.
29. Horton RM, Cai ZL, Ho SN, Pease LR. Gene splicing by overlap extension: tailor-made genes using the polymerase chain reaction. Biotechniques 1990;8: 528–35.
30. Ho EL, Carayannopoulos LN, Poursine-Laurent J, et al. Costimulation of multiple NK cell activation receptors by NKG2D. J Immunol 2002;169:3667–75.
31. Masuda H, Saeki Y, Nomura M, et al. High levels of RAE-1 isoforms on mouse tumor cell lines assessed by anti-"pan" RAE-1 antibody confer tumor susceptibility to NK cells. Biochem Biophys Res Commun 2002; 290:140–5.
32. Salih HR, Goehlsdorf D, Steinle A. Release of MICB molecules by tumor cells: mechanism and soluble MICB in sera of cancer patients. Hum Immunol 2006; 67:188–95.
33. Kaiser BK, Yim D, Chow IT, et al. Disulphide-isomerase-enabled shedding of tumour-associated NKG2D ligands. Nature 2007;447:482–6.
34. Wu J, Chalupny NJ, Manley TJ, Riddell SR, Cosman D, Spies T. Intracellular retention of the MHC class I-related chain B ligand of NKG2D by the human cytomegalovirus UL16 glycoprotein. J Immunol 2003;170:4196–200.
35. Ogasawara K, Hamerman JA, Hsin H, et al. Impairment of NK cell function by NKG2D modulation in NOD mice. Immunity 2003;18:41–51.
36. Diefenbach A, Raulet DH. The innate immune response to tumors and its role in the induction of T-cell immunity. Immunol Rev 2002;188:9–21.
37. Grossmann ME, Wood M, Celis E. Expression, specificity and immunotherapy potential of prostate-associated genes in murine cell lines. World J Urol 2001;19:365–70.
38. Le Maux Chansac B, Misse D, Richon C, et al. Potentiation of NK cell-mediated cytotoxicity in human lung adenocarcinoma: role of NKG2D-dependent pathway. Int Immunol 2008;20:801–10.
39. Gasser S, Orsulic S, Brown EJ, Raulet DH. The DNA damage pathway regulates innate immune system ligands of the NKG2D receptor. Nature 2005;436: 1186–90.
40. Diefenbach A, Tomasello E, Lucas M, et al. Selective associations with signaling proteins determine stimulatory versus costimulatory activity of NKG2D. Nat Immunol 2002;3:1142–9.
41. Zompi S, Hamerman JA, Ogasawara K, et al. NKG2D triggers cytotoxicity in mouse NK cells lacking DAP12 or Syk family kinases. Nat Immunol 2003;4: 565–72.

Immunogenetics (2009) 61:371–384
DOI 10.1007/s00251-009-0368-9

ORIGINAL PAPER

Regulator of complement activation (RCA) gene cluster in *Xenopus tropicalis*

Hiroyuki Oshiumi · Yuzuru Suzuki · Misako Matsumoto · Tsukasa Seya

Received: 19 January 2009 / Accepted: 16 March 2009 / Published online: 25 March 2009

Abstract Genome and expressed sequence tag information of *Xenopus tropicalis* suggested that short-consensus repeat (SCR)-containing proteins are encoded by three genes that are mapped within a 300-kb downstream of *PFKFB2*, which is a marker gene for the regulator of complement activation (RCA) loci in human and chicken. Based on this observation, we cloned the three cDNAs of these proteins using 3′- or 5′-RACE technique. Since their primary structures and locations of the proximity to the *PFKFB2* locus, we named them amphibian RCA protein (ARC) 1, 2, and 3. Expression in human HEK293 or CHO cells suggested that ARC1 is a soluble protein of Mr ~67 kDa, ARC2 is a membrane protein with Mr 44 kDa, and ARC3 a secretary protein with a putative transmembrane region. They were *N*-glycosylated during maturation. In human and chicken RCA clusters, the order in which genes for soluble, GPI-anchored, and membrane forms of SCR proteins are arranged is from the distant to proximity to the *PFKFB2* gene. However, the amphibian ARC1, 2, and 3 resembled one another and did not reflect the same order found in human and chicken RCA genes. This may be due to self-duplication of ARCs to form a family, and it evolved after the amphibia separated from the ancestor of the amniotes, which possessed soluble, GPI-anchored, and membrane forms of SCR protein members. Taken together, frog possesses a RCA locus, but the constitution of the ARC proteins differs from that of the amniotes with a unique self-resemblance.

Keywords Regulator of complement activation (RCA) · Evolution · Gene cluster · Complement · Innate immunity · Amphibia

H. Oshiumi · Y. Suzuki · M. Matsumoto · T. Seya (✉)
Department of Microbiology and Immunology,
Graduate School of Medicine, Hokkaido University,
Kita-ku,
Sapporo 060-8638, Japan
e-mail: seya-tu@pop.med.hokudai.ac.jp

Present address:
Y. Suzuki
NISSUI Pharmaceutical Co. Ltd. 3-23-9,
Ueno, Taito-ku,
Tokyo 110-8736, Japan

Introduction

The complement system consists of effectors for foreign cell clearance and regulators for host cell protection (Morgan and Harris 1999). This innate system primarily functions for host defense against foreign pathogens by highlighting target to eliminate (Morgan and Harris 1999). The active fragment C3b of the third component of complement C3 is a main targeting effector conducting complement-mediated host immune response (Morgan and Harris 1999). The effector system is the protease cascade that activates this pivotal membrane-targeting component C3 by cleaving it into C3b and C3a (Morgan and Harris 1999). The active form C3b covalently binds bacterial membrane to alert the presence of invading foreign material to host immune cells (Morgan and Harris 1999). Additional response following C3b deposition is the assembly of membrane attack by hydrophobic molecular association of pore-forming C5b-9 unit (Morgan and Harris 1999). The C3-activating effector scheme is conserved as similar plasma protease system in most of deuterostomes and a part of protostomes (Nonaka and Kimura 2006; Zhu et al. 2005).

Excessive C3 activation often induces consumption of the complement system and damages self tissue, a type of allergy (Morgan and Harris 1999). The C3-step regulatory system has been identified as a family of multifarious proteins with tandemly repeated ~60 amino acid short consensus repeats (SCRs) (Liszewski et al. 1991). The genes of SCR proteins are clustered at 1q32 called regulator of complement activation (RCA) gene locus in human (Carroll et al. 1988; Liszewski et al. 1991; Rey-Campos et al. 1988). Similar but two split loci of the RCA is found in the mouse (Kingsmore et al. 1989). Furthermore, we found the RCA gene locus with at least four SCR protein genes in the chicken genome (Inoue et al. 2001; Oshiumi et al. 2005). Taken together, the complement regulatory system appears to have developed to diverge into fluid-phase and membrane-bound entities to cope with activation of the complement system. However, phylogenic analysis of the regulatory system is poorly accomplished so far. Our unpublished data show that fish and lamprey possess a single gene encoding a soluble SCR protein in the locus corresponding to the human RCA. Thus, the constituents of the RCA cluster appear different across the vertebrates.

Here, we identified three genes of putative SCR proteins in the *Xenopus tropicalis* genome. Of these, one is a representative membrane-associated complement regulatory protein. This is the first report on the RCA cluster of amphibia, which may reflect the most ancient form of the cluster of complement regulatory proteins.

Material and methods

Cells and tissues

X. tropicalis was a gift from the National Bio-Resource Project (NBRP) of the MEXT, Japan. Fresh *Xenopus* organs were isolated from the individual live frogs and then frozen with liquid nitrogen. All samples were stored at –80°C immediately after collection until use. *Xenopus* blood was collected from the heart by a catheter, and serum was harvested from clotted blood after centrifugation. The human cervical epithelial cell line (HeLa) and Chinese hamster ovary (CHO) cells were obtained from American Type Culture Collection (ATCC, Manassas, VA, USA). HEK293FT (human epithelial kidney) cells were obtained from RIKEN Cell Bank (Wako Pure Chemicals, Saitama, Japan). CHO cells were maintained in Ham's F12/10% fetal calf serum (FCS). HeLa and HEK293FT cells were cultured in MEM/10% FCS and DMEM/10% FCS, respectively. These cells were transfected with cDNAs in expression vectors using the FuGENE HD reagent (Roche) according to manufacture protocol. In some experiments, serum-free medium (Wako Biochemicals, Tokyo, Japan) was used for cell culture, and the supernatants were stored as the source for harvesting transfected gene products in addition to the cell lysates (Kimura et al. 2004). RNaseH was supplied by Promega, Madison WI, USA. ExTaq polymerase was obtained from Takara Bio USA. Marathon cDNA amplification kit was from Clonetech (Palo Alto, CA, USA). FuGENE HD was from Roche Biochemical (Nutely, NJ, USA), and G-Sepahrose was from GE Health care, Madison WI, USA. Block Ace was supplied by Yukijirushi, Sapporo, Japan. Anti-rabbit IGg was obtained from Cappel Laboratories, Cochranville, PA, USA. Neuraminidase and *O*-glycosidase were from Sigmachemical company, St. Louis, MO, USA and Genayme from Cambridege, MA USA.

Isolation of mRNA and RT-PCR

Total RNA was extracted from *Xenopus* tissues and cell lines with TRIZOL reagent (Invitrogen) according to manufacture protocol. Four micrograms of total RNA was reverse-transcribed using RNaseH(−) reverse transcriptase and then subjected to 2 min denaturation at 94°C followed by polymerase chain reaction (PCR) cycle of cDNA amplification using ExTaq polymerase for 35 cycle at 94° C 1 min, annealing at 55°C for 1 min followed by 2 min extension at 72°C. The forward and reverse primers used are described in the following section. The products were separated on 1.5 % agarose gels in TAE and identified by ethidium bromide stain.

Cloning of ARC1, 2, and 3

We assembled expressed sequence tag (EST) sequences of ARC1 on the predicted full sequence of ARC1 taken from the DNA database. Primer sequences used for PCR are listed in Table 1. Total RNA extracted from *X. tropicalis* tissues was used as a template for reverse transcriptase (RT)-PCR for obtaining cDNA. For ARC1, ARC1 primers A, B, C, and D were used (Table 1). We obtained several clones of ARC1 cDNA, and chose a perfect clone without containing PCR errors. During the cloning of the C-terminal region of ARC1 with the primer C and D, we happened to find the short and long cDNA fragments. Aligning the sequences of the two cDNA fragments revealed that the short cDNA sequence lacks the region encoding one SCR domain compared to the long cDNA sequence. We determined the exon/intron structure of ARC1 by comparing the long cDNA sequence with the genome sequence and found that the region absent in the short cDNA fragment of ARC1 exactly corresponds to one exon. Therefore, we concluded that the two cDNA fragments were derived from alternative splicing.

The 5′ region of *ARC2* was not found in any EST sequences encoding *ARC2*; therefore, we carried out

Table 1 Primer list in this study

Name	Sequence
ARC1 A	CAA TCC ACC TGA TTC CAA GG
ARC1 B	CAA AAC ATA GAG GA TTT CCC
ARC1 C	ATT CTG TGA CGT ACA AAT GC
ARC1 D	CGC GGC CGC TCA GAA GAA TTT CCC AAG TAC
ARC2 A	TAA GAA GTC TAG GAG GAG G
ARC2 A′	GGA TCA GGC ACC TTC TAC ACC
ARC2 B	GCT CGA GGC CAC CAT GTT TCC ATA TTG CTC CAT CAG G
ARC2 C	CGC GGC CGC TTA AAA CTT TGT ATA AAA TAT TGA CAG TG
ARC3 A	ATG ATT TGC CAT CGA TAG GG
ARC3 A′	AAG CAG TGC TGG AGG AGG TCC
ARC3 B	ATT GGT AAT CGT TCT GCA TAC TGC AC
ARC3 B′	GCA CTA GTG ATG GAA CCT GG
ARC3 C	GGT CGA CGC CAC CAT GCA TTC TCC ATT TAA TAT C
ARC3D	GGG TAC CTT GGT GAT TTG TTT TTG TTG TG
ARC3E	ACG GAA AAT GGA GTA TTT CC
ARC3F	GCG GCC GCT TAC GCA GTG CAA GCT GTA TAT TG
AP1	CCA TCC TAA TAC GAC TCA CTA TAG GGC
AP2	ACT CAC TAT AGG GCT CGA GCG GC

5′ RACE using Marathon cDNA Amplification kit with AP1, AP2, ARC2 A′, and *ARC2* A primers (Table 1). Based on the result of sequencing, we finally cloned a cDNA-encoding full length *ARC2* using *ARC2* B and C primers.

The 5′ and 3′ end of *ARC3* ORF was not found in any *ARC3* EST sequences. To determine the full length *ARC3* sequence, we executed 5′ and 3′ RACE using AP1, AP2, ARC3 A, ARC3 A′, ARC3 B, and ARC3 B′ as primers (Table 1). Based on the obtained *ARC3* sequence, we cloned the cDNA encoding the full length *ARC3* ORF with ARC3 C, E, D, and F primers.

The conditions of nested PCR were described in a previous report (Inoue et al. 2001; Oshiumi et al. 2005). These cDNA clones were ligated into the *Xho*/*Not*I site of pEFBOS expression vector with HA-tag at the C-terminal ends.

Immunoprecipitation, SDS-PAGE, and Western blotting

Immunoprecipitation was performed using the supernatants of HEK293FT cells transfected with plasmids by FuGENE HD. After incubation for 24 h at 37°C, 2 ml of the supernatant was incubated with 50 μl of Protein G-Sepharose for 1 h at 4°C to remove nonspecific proteins. The cleared supernatants were mixed with 0.5 μg of rabbit anti-HA antibody (Ab) and 20 μl of Protein G-Sepharose beads. The mixture was incubated for 12 h at 4°C. The beads were washed thrice in the wash buffer [phosphate-buffered saline (PBS)/0.02% NP-40] and the beads were extracted with sodium dodecyl sulfate polyacrylamide gel electrophoresis (SDS-PAGE) sample buffer. The samples were subjected to SDS-PAGE followed by Western blotting as described previously (Kimura et al. 2004).

We detected the secreted ARC proteins from the cell culture supernatant. The HEK293 cells were transfected in six-well plate with the plasmid encoding ARC proteins, using FuGENE HD. After 24 h, 2 ml of the culture medium was collected. To remove proteins that nonspecifically bound the Sepharose beads, we added Proteins G Sepharose (50 μl, prewashed) to the medium, and then the protein G Sepharose-containing medium was rotated at 4°C for 1 h. The medium was centrifuged at 2,000 rpm for 1 min, and the supernatant was moved to a new tube. Anti-HA rabbit polyclonal antibody and prewashed protein G Sepharose were added to the tube, and the tube was rotated at 4°C for 24 h. The protein G Sepharose was collected by centrifugation and then washed three times with wash buffer. The immunoprecipitated samples were extracted with SDS-PAGE sample buffer by boiling for 5 min. The samples was analyzed by SDS-PAGE and visualized by Western blotting. We could detect secreted ARC1 and ARC3 proteins.

Immunofluorescence analysis of transfected cells

HeLa cells expressing HA-tag-labeled ARC proteins were incubated with 100 μl of 2 μg/ml rabbit anti-HA Ab for 1 h at 37°C in PBS containing 1% (*w*/*v*) bovine serum albumin. The cells were washed, incubated with a 1:100 dilution of Alexa-conjugated anti-rabbit IgG Ab for 30 min at 37°C in

PBS containing 10% (*w/v*) Block Ace, washed, and mounted on glass slides in PBS containing 2.3% 1,4-diazabiccyclo-2-octane and 50% glycerol. The stained cells were visualized at ×40 magnification under a FLUOVIEW (Olympus, Tokyo, Japan). Images were captured using the attached computer software, FLUOVIEW.

Deglycosylation analysis

The methods for analyses using deglycosidases were described previously (Kimura et al. 2004). Briefly, transfectants (5×10^6) were solubilized in 50 mM Tris-maleate (pH 8.6) containing 1% Nonidet P-40, 10 mM EDTA, 1 mg/ml iodoacetamide, 1 mM phenylmethylsulfonyl fluoride (PMSF) for *O*-glycosidase analysis. For *N*-glycosidase analysis, the same buffer except 20 mM Tris-maleate (pH 6.0) was used. Solubilized proteins were centrifuged at 15,000 rpm for 30 min at 4°C, the pellets were removed, and the supernatants were incubated with 100 μU of neuraminidase for 1 h at 37°C. Then, the samples were treated with either 250 mU of *N*-glycosidase or 1 mU of *O*-glycosidase for 16 h at 37°C. The samples were subjected to SDS-PAGE followed by immunoblotting. ARC proteins were detected with anti-HA Ab as described above.

Protein domain structure and homology analyses

The domain structures of *Xenopus* proteins were predicted using SMART program (http://smart.embl-heidelberg.de/). Signal peptide was predicted by SignalP program (http://www.cbs.dtu.dk/services/SignalP/) (Emanuelsson et al. 2007) using the hidden Markov or neural network model. Although the hidden Markov model failed to predict the ARC3 signal peptide, the neural network model predicted it. Homologies between *Xenopus* and chicken or human proteins were examined by BLAST search analysis. Homologies among SCR domains were determined by comparing the SCR domains of chicken proteins with those of human proteins using TBLASTN program in NCBI BLAST server and GENETYX-MAC Ver. 11.2.1 (GENETYX) maximum matching program. The *N*-glycosylation sites were predicted using NetNGlyc 1.0 server (http://www.cbs.dtu.dk/services/NetNGlyc/).

Results

RCA locus in *X. tropicalis*

Genes in the RCA locus are closely linked to those of *PFKFB2* in human, mouse, and chicken (Oshiumi et al. 2005). We searched for the RCA locus in the *X. tropicalis* genome (JGI genome server) by in silico analysis using the human PFKFB2 full-length sequence as the probe. A *X. tropicalis* gene sequence similar to that of human *PFKFB2*, but not other family members, was found by TBLASTN search against human genome database. Furthermore, three genes containing putative SCRs were identified in close proximity 3′ to the *PFKFB2* gene (Fig. 1a,c). A majority of the SCR-coding regions in these genes were encoded by single exons. The predicted amino acid sequences of all the three genes contain typical SCRs, similar to human and chicken complement regulatory proteins (Fig. 1b). These properties support the existence of a RCA cluster of complement regulatory proteins in frog in a fashion similar to that of human and chicken (Fig. 1c). We call the RCA of amphibia genes ARC and named them from the proximity to the *PFKFB2* locus, ARC1, ARC2, and ARC3.

We have determined the gene structures including the exon–intron boundaries of these three frog RCA genes (Figs. 1a and 2). The results show that SCR2 of ARC1 and ARC2, and SCR2, SCR3, SCR7, and SCR8 of ARC3 were encoded by split exons (Fig. 1a). The splitting features of SCR2 of ARC 1 and 2 and SCR3 of ARC3 were similar to the functionally essential exons of the human and chicken

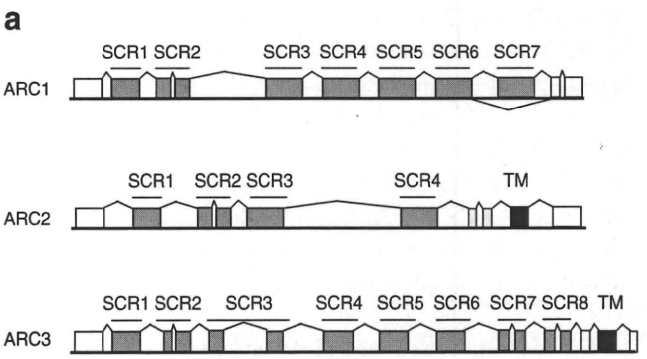

Fig. 1 Identification of three *Xenopus* SCR proteins. **a** Structures of the *X. tropicalis* ARC genes in the genome. The prediction of exon and intron was followed to the JGI database. The ag-gt consensus sequences for splicing are conserved. Non-cording regions and cording regions are represented as *open and grayed rectangles*, respectively. Putative transmembrane (TM) portions are shown as *closed rectangles*. **b** Each SCR sequence of ARC1, 2, and 3 was compared with that of human or chicken SCR proteins using GENETYX ver 11. 2.1 maximum matching program. Regions with high homology are shown as *red* (>45%), *orange* (45~40%), *brown* (40~35%), or *yellow* (30~35%). **c** Comparison of the frog RCA locus with the human and chicken RCA loci. According to the *X. tropicalis* genome sequence, ARC1, 2, and 3 are clustered in the ~300-kbp region, which is longer than the *G. gallus* RCA but shorter than the human RCA locus. The RCA loci of these three species are linked with the PFKFB2 gene, and the gene directions are also conserved. In both human and chicken RCAs, soluble regulators, C4 bp and CRES, are most proximal to PFKFB2, and membrane proteins, MCP and CREM, are most distal to PFKFB2. In *Xenopus*, the soluble protein, ARC1, is most proximal to PFKFB2 gene as human C4 bp and chicken CRES, but unlike human and chicken RCAs, we could not find any GPI-anchored protein in the *Xenopus* RCA locus

Fig. 1 (continued)

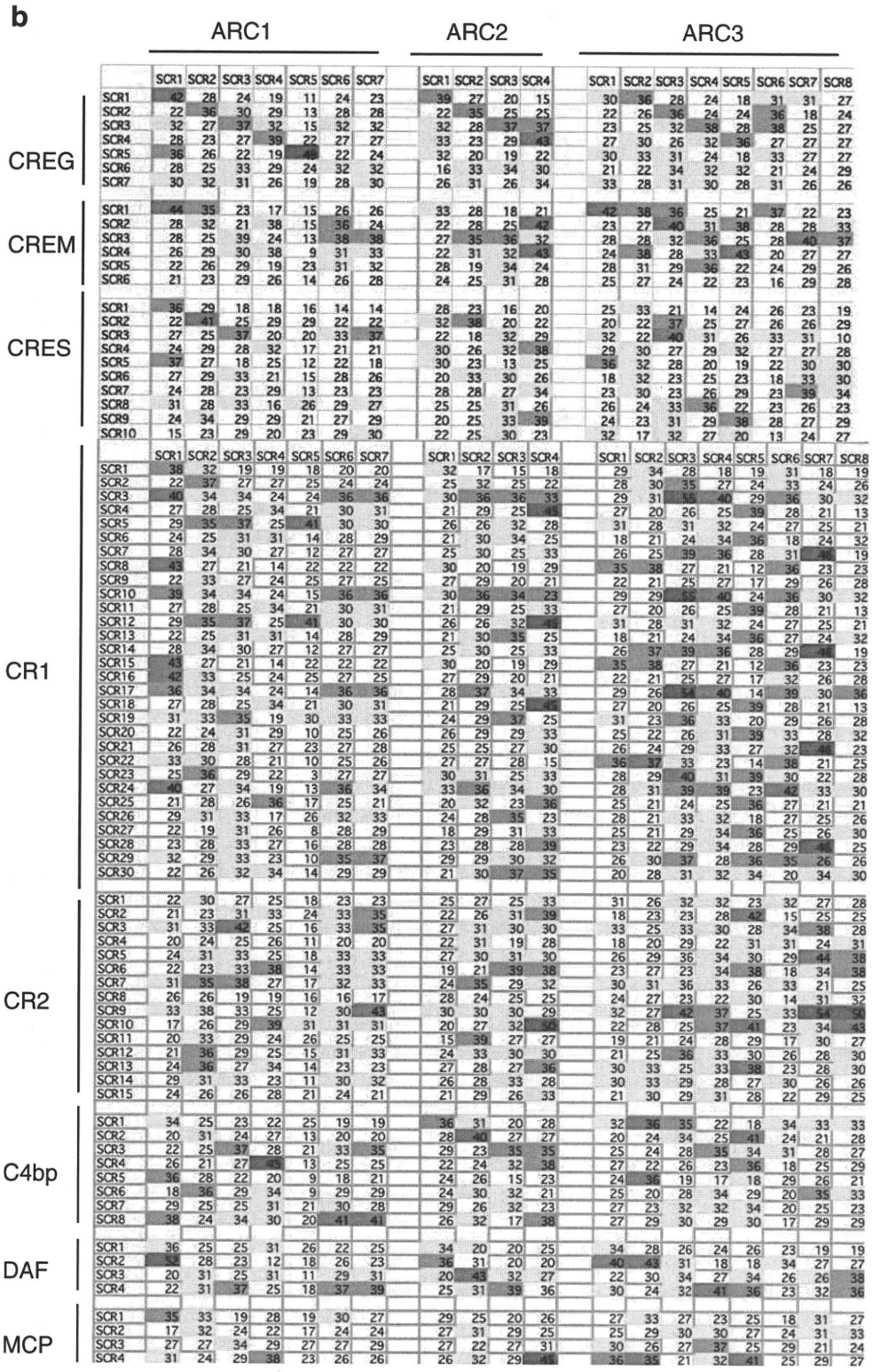

complement regulatory proteins. Furthermore, amino acid sequences of split exon-encoded SCR2 or SCR3 of ARC1, 2, and 3 were highly similar (up to 40%) to those of corresponding functional SCRs of chicken CRES (Fig. 1a, b). Further, the divisions in their coding regions occur at similar positions. However, other chicken RCA proteins CREG and CREM did not show such similarity with ARC proteins (Oshiumi et al. 2005). Thus, it is likely that the split exons in the SCR2 of ARC1/2 and SCR3 of ARC3 encode functionally active domains.

Fig. 1 (continued)

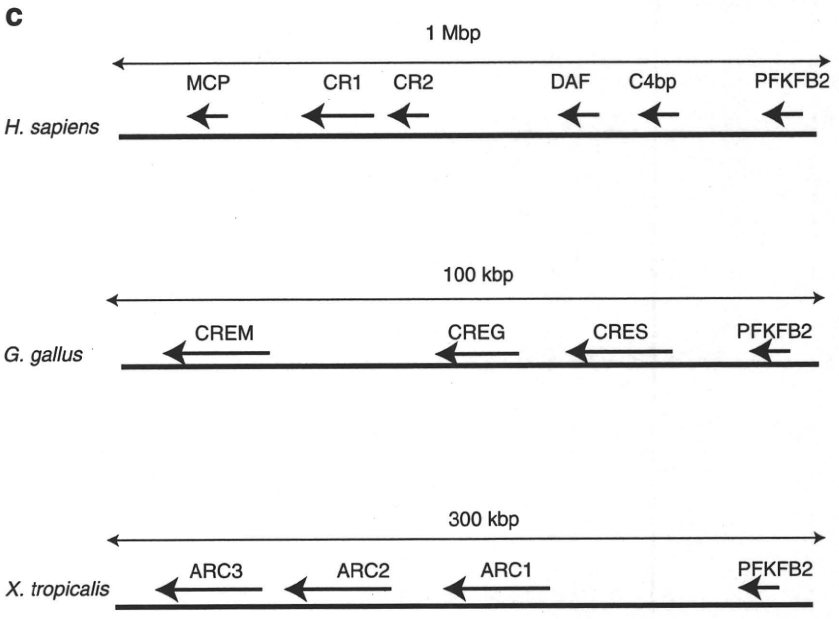

Molecular cloning of ARC1, 2, and 3

EST sequences published covered the whole ORF of *ARC1* and a 3′ part of *ARC2*. *ARC3* EST was only partially identified. In order to obtain the complete ORF of *ARC2*, nested PCR with 5′ RACE was performed. We obtained products whose sequences matched the EST sequences containing an upstream ATG translation initiation and stop codons. To clone the complete *ARC3* cDNA, we performed 5′ and 3′ RACEs and obtained the *ARC3* cDNA sequence containing the 5′ ATG start and the 3′ stop codons. The sequences of *ARC1*, *2*, and *3* are shown in Fig. 2a, b, and c (AB474590, AB474591, AB474592). SignalP analysis suggested that ARC1, ARC2, and perhaps ARC3 have signal sequences. ARC2 and 3 have putative transmembrane regions of ~20 amino acids. The properties of the predicted ARC proteins together with the results of PSORT analysis suggested that ARC1 is a secretary or cytoplasmic protein, while ARC2 and 3 are type I membrane proteins.

From the sequence, ARC1 (later named ARC1L) was found to be 470 amino acid soluble protein with seven SCRs. ARC2 was a 329 amino acid membrane protein with four SCRs, and ARC3 was a 563 amino acid membrane protein with eight SCRs.

Tissue distribution and cellular localization of ARCs

Tissue distribution profiles of these ARC messages were examined by RT-PCR. RNA samples were extracted from the organs indicated and the cDNAs used for templates. Amplifiable sequences of *ARC1* (518–1,447 bp), *ARC2* (1–987 bp), and *ARC3* (1–644 bp) were selected for RT-PCR analysis. We designed PCR primers based on the derived sequences (Table 1). The results showed that the mRNAs of *ARC1* and *3* were ubiquitously expressed, while the *ARC2* mRNA was detected only in the liver, intestine, and muscle (Fig 3a). We found a faster mobility band below the predicted *ARC1* band in all lanes, suggesting the presence of a splicing variant in *ARC1*. The short splicing variant was predicted to encode a protein with six SCRs, which we named ARC1s, as described in the "Materials and methods" section.

We subcloned HA-tagged ARC1L, 2, and 3 using the cloned ARC sequences as templates. When the plasmids were transfected into HEK293FT and CHO cells, the ARC proteins were detected in cell lysates by Western blotting using anti-HA Ab. By confocal analysis using anti-HA Ab, ARC1L and ARC3 were localized to the cytoplasm (Fig. 3b). ARC2 was localized to the cell-surface membrane, supporting the prediction from its amino acid sequence to be a type I membrane protein (Fig. 3b). We

Fig. 2 Complete amino acid sequences of ARC1, 2, and 3. Deduced ▶ amino acid sequences of ARC1 (**a**), ARC2 (**b**), and ARC3 (**c**) are shown under the nucleotide sequences. *Asterisks* indicate the stop codons. The predicted signal sequences are *underlined*. The amino acid sequences with hydrophobicity (putative transmembrane portions) are *double underlined* in ARC2 and 3. The *broken lines* show the position of exon/intron boundaries. The *rectangles* show the predicted N-linked glycosylation Asn residues. The nucleotide sequences have been registered in the EMBL Data Library/GenBank/DDBJ databases with the accession numbers AB474590 (ARC1), AB474591 (ARC2), and AB474592 (ARC3)

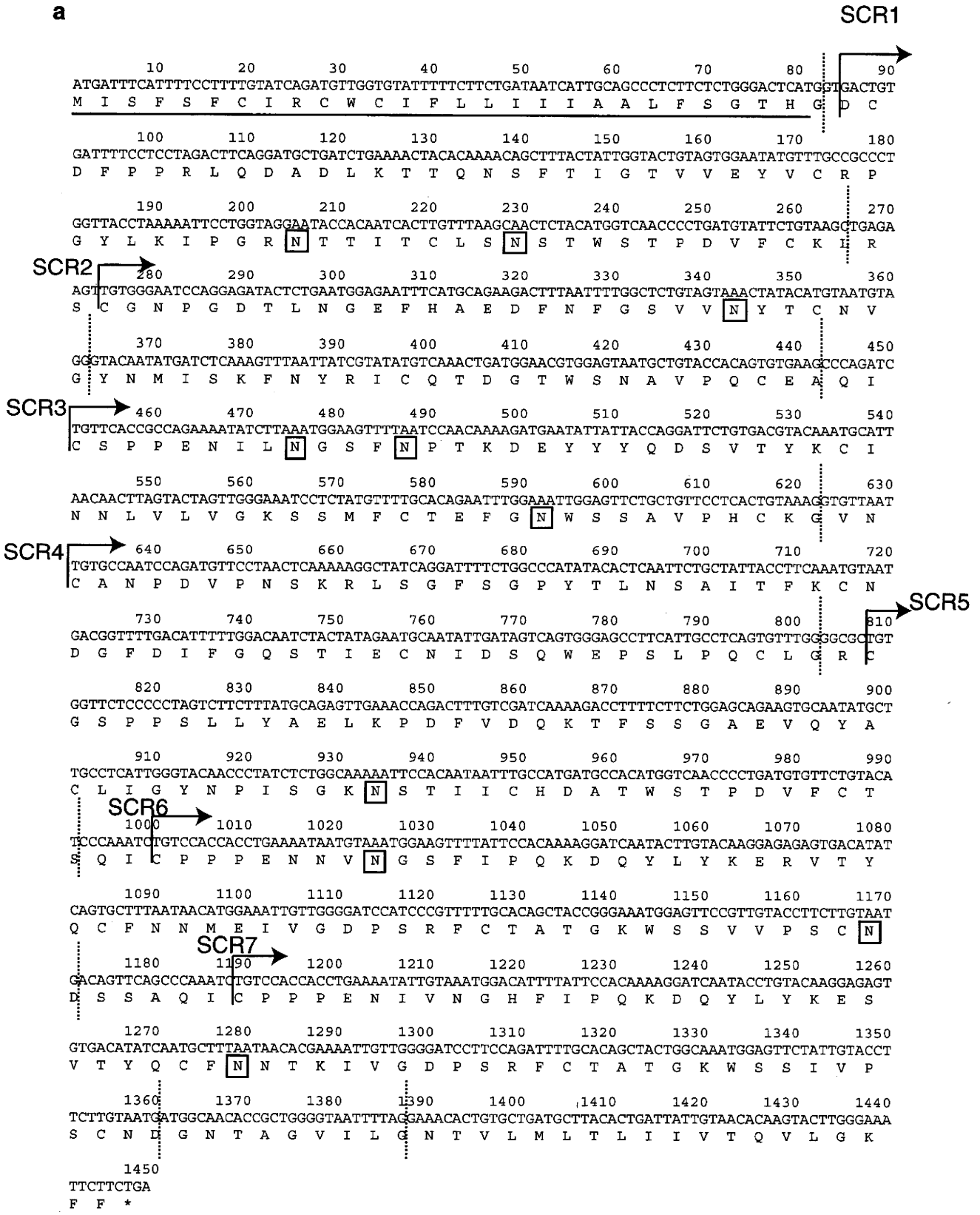
a
SCR1
SCR2
SCR3
SCR4
SCR5
SCR6
SCR7

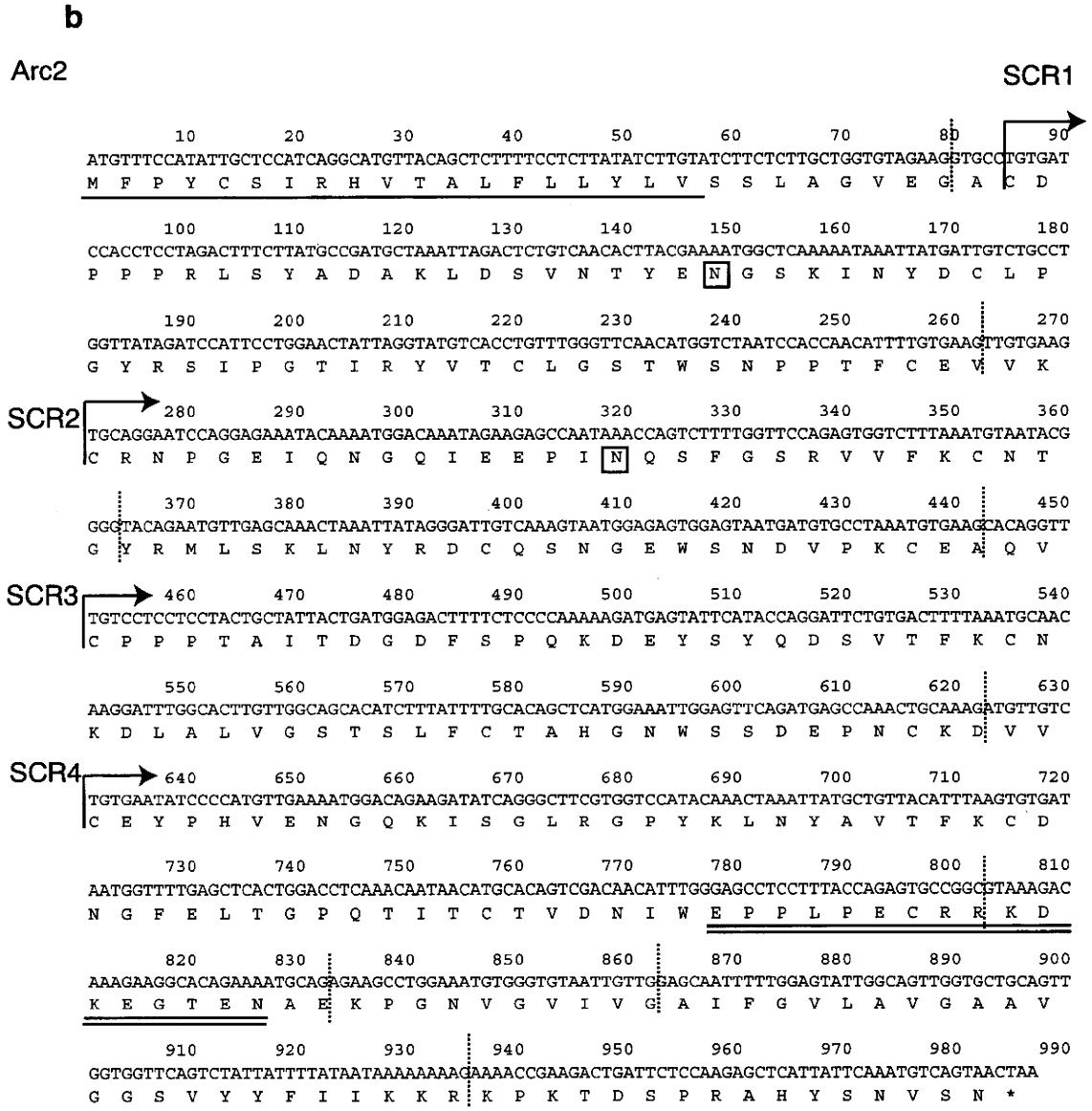

Fig. 2 (continued)

found that the transfected cells secreted ARC1 and 3 proteins into the supernatants. Since the ARC3 protein showed higher molecular weight in the supernatant (75 kDa) than in the cell lysate (70 kDa), it is not yet certain if ARC3 is proteolytically cleaved out from the membrane. ARC3 may retain as an unprocessed form in the cytoplasmic granules and gradually mature during secretion into the media irrespective of the presence of the hydrophobic transmembrane-like sequence.

Posttranslational sugar modification in ARCs

Human complement regulatory proteins often undergo posttranslational sugar modification. Since the molecular masses of the expressed ARC proteins estimated by SDS-PAGE were higher than those predicted from the primary structures, we tested their sugar moieties. *N*-glycosidase treatment of ARC1L (67 kDa), ARC2 (44 kDa), and ARC3 (75 kDa) reduced the molecular masses to 55, 40, and 72 kDa, respectively (Fig. 4). The two band patterns observed in *N*-glycosidase-treated ARC2 and ARC3 may reflect either incomplete sugar digestion or heterogeneous sugar compositions. N-linked sugar modifications of ARC1, 2, and 3 during maturation are also supported by NetNGlyc 1.0 (Julenius et al. 2005; Fig. 2). NetOglyc 3.1 (Blom et al. 2004) analysis did not support the presence of O-linked sugar in ARC proteins. Thus, ARC proteins undergo N-linked sugar modification, which appears to be

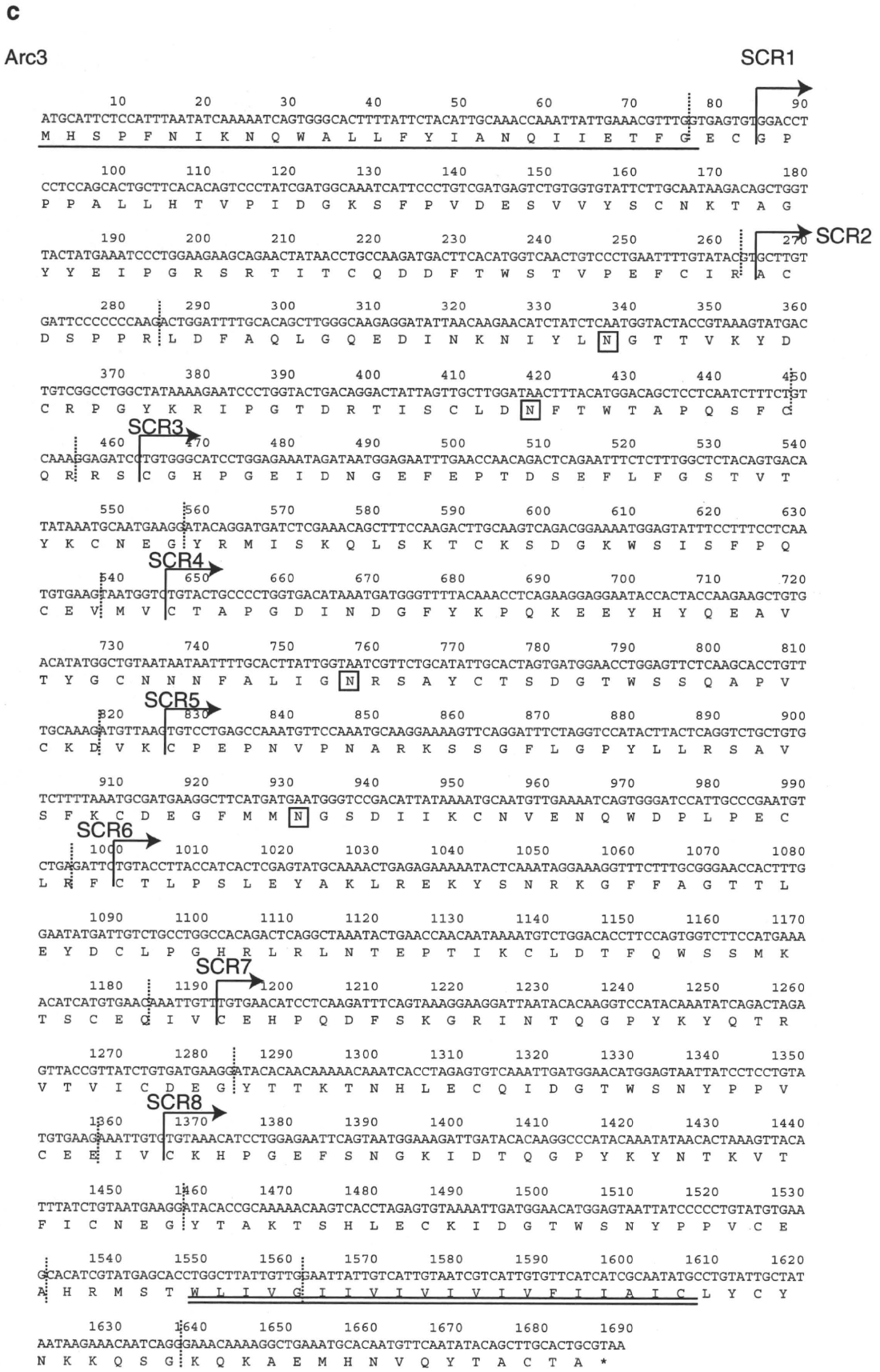

Fig. 2 (continued)

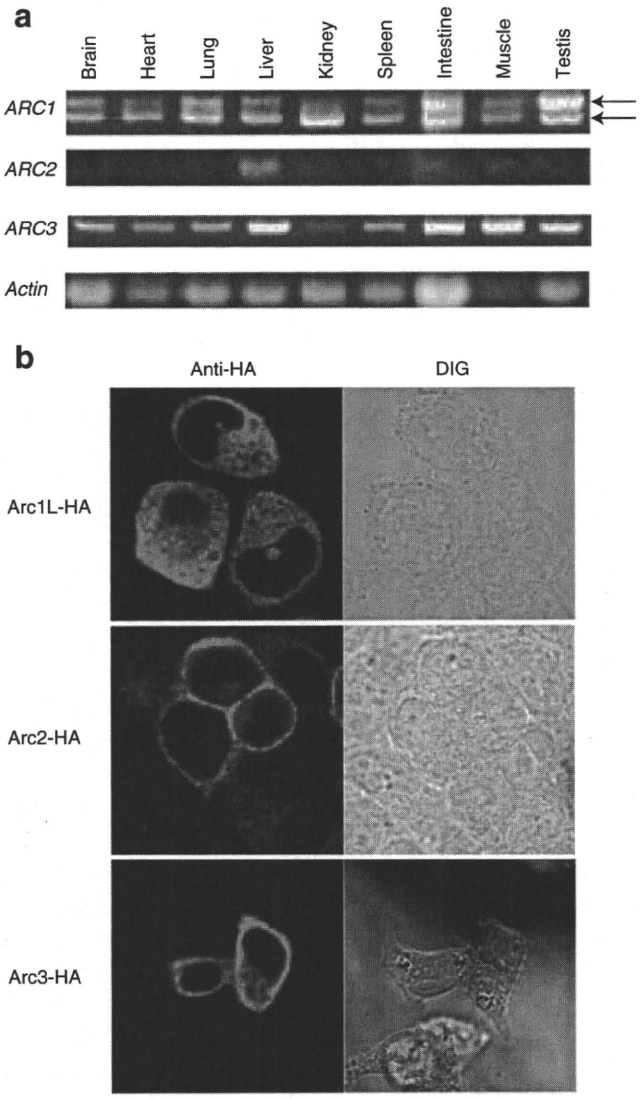

Fig. 3 Expression analyses of the ARC mRNAs in adult frog tissues. **a** RT-PCR analysis. The ARC cDNAs were amplified using the same PCR procedure (see the "Materials and methods" section). Actin was used for a positive control. No product was amplified with the actin cDNA from nonreverse transcribed samples. The experiments were performed by two independent samples, and the representative data is shown. **b** Imaging analysis of ARCs in human cells. HeLa cells expressing HA-tag-labeled ARC proteins were stained with anti-HA Ab and Alexa-conjugated goat anti-rabbit IgG Ab. Cells were fixed and observed with confocal microscope

a process linked to their maturation. On SDS-PAGE, the mature forms of ARC1L (lane 5 of Fig. 4) and ARC3 (lane 13 of Fig. 4) exhibited single bands, but ARC2 showed multiple bands (lane 9 of Fig. 4) reflecting possible multiple modifications for this protein. Interestingly, ARC1L and ARC3 secretary forms have almost identical molecular sizes to their cytoplasmic forms. The mechanism of secretion of ARC3 from transfected cells is yet to be determined.

Phylogenetic analysis of ARCs

Previously, we showed that avian, *Gallus gallus*, RCA genes, CRES, CREM, and CREG, were homologs of C4 bp, MCP, and DAF, respectively (Oshiumi et al. 2005), despite their frequent domain shuffling among those genes. To examine the orthologous relationship between human and amphibian RCA genes, their protein sequences were aligned by ClustalW software, and the phylogenic tree was drawn by neighbor-joining method. Surprisingly, we found that the amphibian ARC1, 2, and 3 are closely related with each other and not clustered to contain any ortholog of the human RCA gene (Fig. 5a). To further confirm that the amphibian RCA proteins are more similar to each other than to human RCA proteins, we carried out BLAST search analyses. The results showed that *ARC1* was more similar to *ARC2* and *3* than human RCA genes. *ARC2* and *3* also resemble more to *ARC1* than human RCA (Table 2). These results support the notion that *X. tropicalis* RCA genes underwent duplication after *X. tropicalis* ancestor had diverged from human and their common ancestor.

The most popular form of the human CR1 protein consists of four tandem repeats of a unit of seven SCR domains (Klickstein et al. 1987). To elucidate whether *X. tropicalis* possesses an SCR repeat-containing gene in the RCA locus similar to that of human CR1, the sequences of each SCR domain of ARCs were compared to each other (Fig. 5b and Table 2). The results showed that almost all SCR domains of *X. tropicalis* RCA proteins could be clustered into four groups. We named these four SCR domains SCR-A, B, C, and D. The order of ARC1 SCR is A-B-C-D-A-C-C (Fig. 5c). In ARC2 protein, there is no duplicate of SCR domain, and its order is A-B-C-D (Fig. 5c). In ARC3, two ambiguous SCR domains follow A-A-B-C-D of SCR domains (Fig. 5c). Because the order, SCR-A-B-C-D, commonly exists in the three ARC proteins, the ancestral ARC protein seems to consist of SCR-A-B-C-D, and the duplication of SCR domains might have occurred in ARC1 and ARC3, but not ARC2. Next, we compared the similarity of ARC SCR-A, B, C, D to human or chicken RCA protein SCRs. Interestingly, the ARC SCRs were similar to DAF or CREG proteins, both of which are GPI-anchored proteins, in that DAF and CREG fundamentally consist of SCR-A-B-C-D. This is reminiscent of the order of SCR-A-B-C-D found in the putative *Xenopus* ARC ancestor (Fig. 1b).

Discussion

Here we demonstrated that *X. tropicalis* possesses three SCR proteins ARC1, 2, and 3. They were mapped

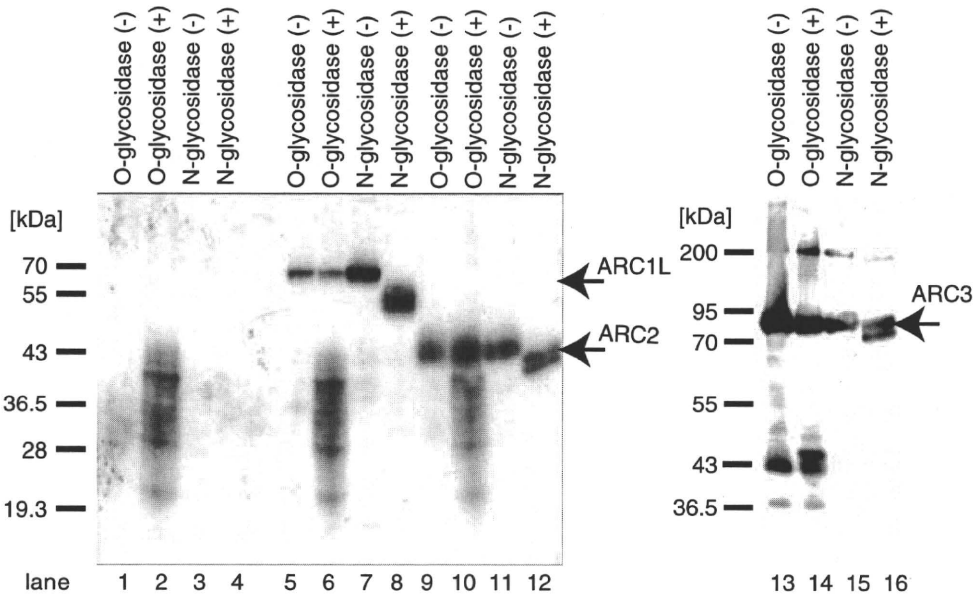

Fig. 4 Deglycosylation analysis of ARCs. Immunoblotting profiles of ARC1, 2, and 3. Cell lysates containing ARC proteins were treated with *N*- or *O*-glycosidase and analyzed on SDS-PAGE and immunoblotting. *Arrows* indicate major bands of ARC1L, ARC2, and ARC3. *lanes 1–4* control with no sample, *lanes 5-8* ARC1L, *lanes 9–12* ARC2; *lanes 13–16* ARC3

downstream of the *PFKFB2* gene, like the RCA loci of human and chicken. In human, group B complement regulatory proteins, C4 bp, DAF, CR2, CR1, and MCP (Krushkal et al. 2000), clustered downstream of *PFKFB2* in chromosome 1q32 (Rey-Campos et al. 1988). In chicken, CRES, CREG, CR1-like undefined gene, and CREM are clustered downstream of *PFKFB2* in a microchromosome (Oshiumi et al. 2005). Thus, the order of soluble, GPI-anchored, and membrane forms of RCA genes is essentially the same in human and chicken. We expected that ARC1, 2, and 3 reflect the order of CRES, CREG, and CREM in chicken. However, ClustalW alignment and expression analyses showed that amphibian ARCs did not follow the conventional organization. The three ARC proteins resemble each other. From these current views, we speculate that ARCs self-duplicated to form a RCA family. The ARC family evolved after the amphibia separated from the ancestor of the homeotherm, which possess soluble, GPI-anchored, and membrane forms of SCR protein members.

Human and chicken RCA products have complement regulatory activity (Morgan and Harris 1999; Oshiumi et al. 2005) by either accelerating the decay of the C3 convertases or cleaving C3b into inactive forms. It is not surprising that the frog ARC proteins possess complement regulatory activity toward the frog C3b and C3 convertases, the presence of which has been reported .(Fujii et al. 1985; Grossberger et al. 1989; Sekizawa et al. 1984). Although the functional point of ARCs needs to be experimentally addressed, gene structure analysis suggested that SCR2 of ARC1 (s and L forms), ARC2, and ARC3 were encoded by split exons similar to those of human/chicken C3-step regulatory proteins. In human RCA proteins, SCR2 play a central role in C3b inactivation (Casasnovas et al. 1999; Liszewski et al. 2000). Hence, the primary composition of SCR2 is conserved across human and frogs.

This study further revealed that frog has a membrane-associated form of RCA proteins. ARC2 and ARC3 possessed transmembrane domains. By overexpression analysis, ARC2 protein was localized to the surface of cell membrane, which confirms the notion that ARC2 is a membrane protein. Many reports suggested that mammals and chicken do possess membrane forms of complement regulatory protein (Morgan and Harris 1999; Oshiumi et al. 2005). However, no report indicated that fish have a membrane SCR protein, although we showed that they have soluble SCR proteins for inhibiting fluid-phase complement activation (Oshiumi and Seya, unpublished data). In fact, teleost fish have single or duplicated genes encoding soluble SCR proteins around the downstream locus of *PFKFB2*. We favor a tentative propose that amphibia are the first vertebrates to possess membrane-associated RCA proteins.

From its structural analysis, we are prone to think that ARC3 could also be a membrane-associated SCR protein which gets clipped by proteolytic cleavage to generate a secreted form. How the ARC3 soluble form naturally generates in human cells remains undetermined. The discrepancy observed in ARC3 cellular vs. soluble proteins needs further analyses.

Since ARC1 and 3 were ubiquitous while ARC2 had limited expression in the liver and intestine, functional divergence might have occurred in amphibian RCA proteins. There are several tyrosine-based motifs in the cytoplasmic tail of ARC2. As its functionality may be